


# Nature of the lowest-lying odd parity charmed baryon $\Lambda_c(2595)$ and $\Lambda_c(2625)$ resonances

J. Nieves  and R. Pavao 

*Instituto de Física Corpuscular (centro mixto CSIC-UV), Institutos de Investigación de Paterna, Apartado 22085, 46071, Valencia, Spain*

 (Received 15 July 2019; published 22 January 2020)

We study the structure of the  $\Lambda_c(2595)$  and  $\Lambda_c(2625)$  resonances in the framework of an effective field theory consistent with heavy quark spin and chiral symmetries, which incorporates the interplay between  $\Sigma_c^{(*)}\pi - ND^{(*)}$  baryon-meson degrees of freedom (d.o.f.) and bare  $P$ -wave  $c\bar{u}d$  quark-model states. We show that these two resonances are not heavy quark spin symmetry partners. The  $J^P = 3/2^-$   $\Lambda_c(2625)$  should be viewed mostly as a dressed three-quark state, whose origin is determined by a bare state, predicted to lie very close to the mass of the resonance. The  $J^P = 1/2^-$   $\Lambda_c(2595)$  seems to have, however, a predominant molecular structure. This is because it is either the result of the chiral  $\Sigma_c\pi$  interaction, whose threshold is located much closer than the mass of the bare three-quark state, or because the light d.o.f. in its inner structure are coupled to the unnatural  $0^-$  quantum numbers. We show that both situations can occur depending on the renormalization procedure used. We find some additional states, but the classification of the spectrum in terms of heavy quark spin symmetry is difficult, despite having used interactions that respect this symmetry. This is because the bare quark-model state and the  $\Sigma_c\pi$  threshold are located extraordinarily close to the  $\Lambda_c(2625)$  and  $\Lambda_c(2595)$ , respectively, and hence they play totally different roles in each sector.

DOI: [10.1103/PhysRevD.101.014018](https://doi.org/10.1103/PhysRevD.101.014018)

## I. INTRODUCTION

In the infinite quark mass limit ( $m_Q \rightarrow \infty$ ), the dynamics of baryons containing a heavy quark should show an SU(2) pattern because of the symmetry that quantum chromodynamics (QCD) acquires in that limit under arbitrary rotations of the spin of the heavy quark,  $S_Q$ . This is known as heavy quark spin symmetry (HQSS) [1–3]. The total angular momentum  $j_{ldof}$  of the light degrees of freedom ( $ldof$ ) inside of the hadron is conserved, and heavy baryons with  $J = j_{ldof} \pm 1/2$  are expected to form a degenerate doublet.

Constituent quark models (CQMs) find a nearly degenerate pair of  $P$ -wave  $\Lambda_c^*$  excited states, with spin-parity  $J^P = 1/2^-$  and  $3/2^-$ , and masses similar to those of the isoscalar odd parity  $\Lambda_c(2595)$  and  $\Lambda_c(2625)$  resonances [4–8]. Two different excitation modes are generally considered. In the  $\lambda$  mode, excitations between the heavy quark and the  $ldof$  are accounted for, while in the  $\rho$  mode, excitations in the inner structure of the  $ldof$  are instead

considered. For singly heavy baryons, the typical excitation energies of the  $\lambda$  mode are smaller than those of the  $\rho$  mode [8,9]. Within this picture, the  $\Lambda_c^{\text{CQM}}(2595)$  and  $\Lambda_c^{\text{CQM}}(2625)$  resonances would correspond to the members of the HQSS doublet associated to  $(\ell_\lambda = 1, \ell_\rho = 0)$ , with total spin  $S_q = 0$  for the  $ldof$ . The total spins of these states are the result of coupling the orbital-angular momentum  $\ell_\lambda$  of the  $ldof$ —with respect to the heavy quark—with  $S_Q$ . Therefore, both  $\Lambda_c^{\text{CQM}}(2595)$  and  $\Lambda_c^{\text{CQM}}(2625)$  states are connected by a simple rotation of the heavy-quark spin, and these resonances will be degenerate in the  $m_Q \rightarrow \infty$  limit.

Since the total angular momentum and parity of the  $ldof$  in the  $S$ -wave  $\Sigma_c\pi$  and  $\Sigma_c^*\pi$  pairs are  $1^-$ , as in the CQM  $\Lambda_c(2595)$  and  $\Lambda_c(2625)$  resonances, the  $\Lambda_c^{\text{CQM}}(2595, 2625) \rightarrow \pi\Sigma_c^{(*)} \rightarrow \pi\pi\Lambda_c$  decays respect HQSS, and hence one could expect sizable widths for these resonances, unless these transitions are kinematically suppressed. This turns out to be precisely the case [10], and as it is shown in Refs. [11,12], the use of the actual resonance masses lead to widths for the CQM  $(\ell_\lambda = 1, \ell_\rho = 0)$  states ( $j_{ldof}^\pi = 1^-$ ) predicted in [8], which is consistent with data.

Within CQM schemes, it is nevertheless unclear why the role played by the  $\Sigma_c^{(*)}\pi$  baryon-meson pairs in the generation of the  $\Lambda_c(2595)$  and  $\Lambda_c(2625)$  resonances can be safely ignored, especially in the  $\Lambda_c(2595)$  case,

*Published by the American Physical Society under the terms of the Creative Commons Attribution 4.0 International license. Further distribution of this work must maintain attribution to the author(s) and the published article's title, journal citation, and DOI. Funded by SCOAP<sup>3</sup>.*

since it is located very close to the  $\Sigma_c\pi$  threshold (1 MeV below or 4 MeV above, depending on the charged channel). This observation leads us naturally to consider molecular descriptions of these lowest-lying odd parity charmed baryon states, which should show up as poles in coupled-channel  $T$  matrices, fulfilling exact unitarity.

The first molecular studies [13,14] of the  $\Lambda_c(2595)$  and  $\Lambda_c(2625)$  were motivated by the appealing similitude of these resonances to the  $\Lambda(1405)$  and  $\Lambda(1520)$  in the strange sector. In particular, the two isoscalar  $S$ -wave  $\Lambda(1405)$  and  $\Lambda_c(2595)$  resonances have several features in common. The mass of the former lies in between the  $\Sigma\pi$  and  $N\bar{K}$  thresholds, to which it couples strongly. In turn, the  $\Lambda_c(2595)$  lies below the  $ND$  and just slightly above the  $\Sigma_c\pi$  thresholds, and substituting the  $c$  quark by an  $s$  quark, one might expect the interaction of  $ND$  to play a role in the dynamics of the  $\Lambda_c(2595)$  similar to that played by  $N\bar{K}$  in the strange sector. The first works had some clear limitations. The  $J^P = 1/2^-$  sector was studied in [13], where the amplitudes obtained from the scattering of Goldstone bosons off  $1/2^+$  heavy-light baryons were unitarized. Despite the interactions being fully consistent with chiral symmetry, neither the  $ND$  nor the  $ND^*$  channels were considered.<sup>1</sup> The work of Ref. [14] also studied the  $\Lambda_c(2595)$  and there, the interactions were obtained from chirally motivated Lagrangians upon replacing the  $s$  quark by the  $c$  quark. Though in this way, the  $ND$  channel was accounted for, the HQSS counterpart  $ND^*$  was not considered. Subsequent works [16–19] introduced some improvements, but they failed to provide a scheme fully consistent with HQSS. In all cases, the  $\Lambda_c(2595)$ , or the  $\Lambda_c(2625)$  when studied, could be dynamically generated after a convenient tuning of the low energy constants (LEC) needed to renormalize the ultraviolet (UV) divergences resulting from the baryon-meson loops. As mentioned before, none of these works were consistent with HQSS since none of them considered the  $ND^*$  channel [20]. Heavy pseudoscalar and vector mesons should be treated on equal footing, since they are degenerated in the heavy quark limit, and are connected by a spin rotation of the heavy quark that leaves unaltered the QCD Hamiltonian in that limit.

The first molecular description of the  $\Lambda_c(2595)$  and  $\Lambda_c(2625)$  resonances, using interactions fully consistent with HQSS, was proposed in Refs. [20,21]. In these works, a consistent  $SU(6)_{\text{lsf}} \times SU(2)_{\text{HQSS}}$  extension of the chiral Weinberg-Tomozawa (WT)  $\pi N$  Lagrangian—where “lsf” stands for light-spin-flavor symmetry—was derived. Two states with  $J^P = 1/2^-$  were dynamically generated in the

<sup>1</sup>A detailed treatment of the interactions between the ground state  $1/2^+$  and  $3/2^+$  singly charmed and bottomed baryons and the pseudo-Nambu-Goldstone bosons, discussing also the effects of the next-to-leading-order chiral potentials, can be found in [15].

region of 2595 MeV. The first one, identified with the  $\Lambda_c(2595)$  resonance, was narrow and it strongly coupled to  $ND$  and especially to  $ND^*$ , with a small coupling to the open  $\Sigma_c\pi$  channel. Its wave function had a large  $j_{\text{dof}}^\pi = 0^-$  component that, coupled to the spin ( $S_Q = \frac{1}{2}$ ) of the charm quark, gives a total  $J^P = \frac{1}{2}^-$  for the  $\Lambda_c(2595)$ . Since the transition of the dominant  $j_q^P = 0^-$  term of the  $\Lambda_c(2595)$  to the final  $\Sigma_c\pi$  state is forbidden by HQSS, this mechanism will act in addition to any possible kinematical suppression.

The second  $J^P = 1/2^-$  state found in [20,21] was quite broad since it had a sizable coupling to the  $\Sigma_c\pi$  channel, and reproduced, in the charm sector, the chiral two-pole structure of the  $\Lambda(1405)$  [22–28]. On the other hand, a  $J^P = 3/2^-$  state is generated mainly by the  $(ND^* - \Sigma_c^*\pi)$  coupled-channel dynamics. It would be the charm counterpart of the  $\Lambda(1520)$ , and it was argued that this could be identified with the  $\Lambda_c(2625)$  resonance.

Several  $\Lambda_c^*$  poles were also obtained in the approach followed in Ref. [29]. There, the interaction of  $ND$  and  $ND^*$  states, together with their coupled channels, are considered by using an extension of the  $SU(3)$  local hidden gauge formalism from the light meson sector [30–32] to four flavors. The scheme also respects leading-order HQSS constraints [33] and, as in Refs. [20,21], a two-pole structure for the  $\Lambda_c(2595)$  was also found, with the  $ND^*$  channel playing a crucial role in its dynamics. This is a notable difference to the situation in the strange sector, where the analog  $N\bar{K}^*$  channel is not even considered in most of the studies of the  $\Lambda(1405)$ , because of the large  $\bar{K}^* - \bar{K}$  mass splitting. We will refer to this model as extended local hidden gauge (ELHG) for the rest of this work.

However, neither the  $SU(6)_{\text{lsf}} \times SU(2)_{\text{HQSS}}$  model, nor the ELHG, consider the interplay between  $\Sigma_c^{(*)}\pi - ND^{(*)}$  baryon-meson d.o.f. and bare  $P$ -wave  $c\bar{u}d$  quark-model states. This is unjustified, in the same way it was also unjustified in the neglect of baryon-meson effects in the CQM approaches.

The CQM approach of Ref. [8] finds isoscalar  $J^P = 1/2^-$  and  $3/2^-$  states at 2628 and 2630 MeV, respectively. Given the proximity of these bare three-quarks states to the  $\Lambda_c(2595)$  and  $\Lambda_c(2625)$ , it is reasonable to expect a significant influence of the CQM d.o.f. on the dynamics of the physical states. This seems to be especially true for the  $\Lambda_c(2625)$ , for which the CQM prediction almost matches its mass. CQM d.o.f. can be taken into account in hadron scattering schemes by considering an additional energy dependent interaction [34,35], driven by a pole in the baryon-meson tree-level amplitudes located at the bare mass,  $\overset{\circ}{M}_{\text{CQM}}$ , of the CQM state. At energies far enough from  $\overset{\circ}{M}_{\text{CQM}}$ , the contribution of the CQM d.o.f. can be possibly accounted for by an appropriate LEC (induced by the UV regulator of the loops) in the unitarized baryon-meson amplitude. However, such a contribution becomes

more important for energies approaching  $\overset{\circ}{M}_{\text{CQM}}$ , and its energy dependence might then not be safely ignored.

In this work, we will study of the structure of the  $\Lambda_c(2595)$  and  $\Lambda_c(2625)$  resonances, in the framework of an effective theory consistent with heavy quark spin and chiral symmetries, incorporating for the very first time, the interplay between  $\Sigma_c^{(*)}\pi - ND^{(*)}$  baryon-meson d.o.f. and bare  $P$ -wave  $c\bar{u}d$  quark-model states. For simplicity, we will use the  $\text{SU}(6)_{\text{lsf}} \times \text{HQSS}$  baryon-meson amplitudes, though the most important conclusions extracted here do not depend on the particular hadron scattering model employed.

The work is organized as follows. After this Introduction, the used formalism is briefly revised in Sec. II, which is split into several subsections dealing with the  $\text{SU}(6)_{\text{lsf}} \times \text{HQSS}$  hadron amplitudes, their renormalization and structure in the complex plane, with the inclusion of the CQM d.o.f., and finally with the evaluation of the  $\Lambda_c^*(1/2^-, 3/2) \rightarrow \Lambda_c(1/2^+)\pi\pi$  three-body decays. The results of this research are presented and discussed in Sec. III, first neglecting CQM effects (Sec. III A) and next coupling CQM and baryon-meson d.o.f. (Sec. III B). Finally, the main conclusions of this work are summarized in Sec. IV.

## II. FORMALISM

### A. $\text{SU}(6)_{\text{lsf}} \times \text{HQSS}$ amplitudes

The building blocks considered in [20,21,36] in the  $C=1$  sector are the pseudoscalar ( $D_s, D, K, \pi, \eta, \bar{K}, \bar{D}, \bar{D}_s$ ) and vector ( $D_s^*, D^*, K^*, \rho, \omega, \bar{K}^*, \bar{D}^*, \bar{D}_s^*, \phi$ ) mesons, the spin-1/2 octet and the spin-3/2 decuplet of low-lying light baryons, in addition to the spin-1/2 ( $\Lambda_c, \Sigma_c, \Xi_c, \Xi_c', \Omega_c$ ), and spin-3/2 ( $\Sigma_c^*, \Xi_c^*, \Omega_c^*$ ) charmed baryons. All baryon-meson pairs with ( $C=1, S=0, I=0$ ) quantum numbers span the coupled-channel space for a given total angular momentum  $J$  and odd parity. The  $S$ -wave tree-level amplitudes between two channels are given by the  $\text{SU}(6)_{\text{lsf}} \times \text{HQSS}$  WT kernel

$$V_{ij}^J(s) = D_{ij}^J \frac{2\sqrt{s} - M_i - M_j}{4f_i f_j} \sqrt{\frac{E_i + M_i}{2M_i}} \sqrt{\frac{E_j + M_j}{2M_j}}, \quad (1)$$

with  $s$  the baryon-meson Mandelstam variable,  $M_i$  and  $m_i$ , the masses of the baryon and meson in the  $i$  channel, respectively, and  $E_i = (s - m_i^2 + M_i^2)/2\sqrt{s}$ , the center-of-mass energy of the baryon in the same channel. The hadron masses and meson decay constants,  $f_i$ , have been taken from Ref. [21]. The  $D_{ij}^J$  matrices are determined by the underlying  $\text{SU}(6)_{\text{lsf}} \times \text{HQSS}$  group structure of the interaction. Tables for all of them can be found in Appendix B of Ref. [20]. Here, we truncate the coupled-channels space to that generated by the  $\Sigma_c\pi, ND$ , and  $ND^*$  and  $\Sigma_c^*\pi$  and  $ND^*$  in the  $J^P = 1/2^-$  and  $3/2^-$  sectors, respectively.

Other higher channels like  $\Lambda_c\eta, \Lambda_c\omega, \Xi_c^{(\prime,*)}K^{(*)}, \Lambda D_s^{(*)}, \Sigma_c^{(*)}\rho, \dots$  are somewhat relevant for the dynamics of the  $\Lambda_c(2595)$  and  $\Lambda_c(2625)$  resonances [20,21], and have not been considered in the analysis carried out in this work.

The matrices  $D^J$  are given in [20] in a basis of  $S$ -wave baryon-meson states. They become, however, diagonal when states with well-defined  $ldof$  total angular momentum,  $j_{ldof}$ , are used. For the latter states, HQSS constrains are straightforward because of the symmetry that QCD acquires, in the infinite quark mass limit, under arbitrary rotations of the spin of the heavy quark [1–3]. In both bases, the total angular momentum of the baryon-meson pair is defined, and both sets of states are related by a Racah rotation [33,37]. In the  $(\Sigma_c^{(*)}\pi, ND^{(*)})$  truncated space, these matrices read

$$D^{J=1/2} = \begin{array}{c} \Sigma_c\pi \quad ND \quad ND^* \\ \left( \begin{array}{ccc} -4 & \sqrt{3/2} & -1/\sqrt{2} \\ \sqrt{3/2} & -3 & -3\sqrt{3} \\ -1/\sqrt{2} & -3\sqrt{3} & -9 \end{array} \right) \\ \Sigma_c^*\pi \quad ND^* \end{array} \quad (2)$$

$$D^{J=3/2} = \begin{array}{c} \Sigma_c\pi \quad ND^* \\ \left( \begin{array}{cc} -4 & -\sqrt{2} \\ -\sqrt{2} & 0 \end{array} \right) \end{array}$$

with eigenvalues  $\lambda_0 = -12$ ,  $\lambda_1^{\text{atr}} = -2 - \sqrt{6}$ , and  $\lambda_1^{\text{rep}} = -2 + \sqrt{6}$ , and  $\lambda_1^{\text{atr}}$  and  $\lambda_1^{\text{rep}}$ , for  $J^P = 1/2^-$  and  $J^P = 3/2^-$ , respectively [37]. Actually, the  $\text{SU}(6)_{\text{lsf}} \times \text{SU}(2)_{\text{HQSS}}$  extension of the WT  $\pi N$  interaction proposed in [20,21,36] leads to a large attraction ( $\lambda_0$ ) in the subspace where the total angular-momentum-parity quantum numbers of the  $ldof$  are  $j_{ldof}^\pi = 0^-$ . This latter configuration does not occur for  $J = 3/2$ , when only  $S$ -wave interactions are considered, and the  $ldof$  are necessarily coupled to  $j_{ldof}^\pi = 1^-$ . In the  $j_{ldof}^\pi = 1^-$ -subspace, there exist both attractive ( $\lambda_1^{\text{atr}}$ ) and repulsive ( $\lambda_1^{\text{rep}}$ ) components, and HQSS relates the  $D^{J=1/2}$  and  $D^{J=3/2}$  matrices.

In summary, the  $D^J$  matrices of Eq. (2) are fully consistent with HQSS, as explicitly discussed in Sec. 2.2 of Ref. [37]. In addition, some spin-flavor symmetry breaking terms are included in the approach, as in Refs. [20,21], by employing physical hadron masses and decay constants. This induces mostly  $\text{SU}(4)$ -flavor breaking corrections, since the charmed-hadrons masses and decay constants follow the HQSS predictions in good approximation.

### B. Renormalization of the Bethe-Salpeter equation

We use the matrix  $V_{ij}^J$  as a kernel to solve the Bethe-Salpeter equation (BSE), leading to a  $T$  matrix

$$T^J(s) = \frac{1}{1 - V^J(s)G^J(s)} V^J(s), \quad (3)$$

satisfying exact unitarity in coupled channels. The diagonal matrix  $G^J(s)$  is constructed out of the baryon-meson loop functions

$$G_i(s) = i2M_i \int \frac{d^4q}{(2\pi)^4} \frac{1}{q^2 - m_i^2 + i\epsilon} \frac{1}{(P - q)^2 - M_i^2 + i\epsilon}, \quad (4)$$

with  $P$  the total momentum of the system such that  $P^2 = s$ . We omit the index  $J$  from here on for simplicity. The bare loop function is logarithmically UV divergent and needs to be renormalized. This can be done by one subtraction

$$G_i(s) = \bar{G}_i(s) + G_i(s_{i+}), \quad (5)$$

where the finite part of the loop function,  $\bar{G}_i(s)$ , reads

$$\bar{G}_i(s) = \frac{2M_i}{(4\pi)^2} \left( \left[ \frac{M_i^2 - m_i^2}{s} - \frac{M_i - m_i}{M_i + m_i} \right] \log \frac{M_i}{m_i} + L_i(s) \right), \quad (6)$$

with  $s_{i\pm} = (m_i \pm M_i)^2$  and the multivalued function  $L(s)$  given in Eq. (A10) of Ref. [38].

The divergent contribution of the loop function,  $G_i(s_{i+})$  in Eq. (5), needs to be renormalized. We will examine here two different renormalization schemes. On the one hand, we will perform one subtraction at a certain scale  $\sqrt{s} = \mu$ , such that  $G_i(\sqrt{s} = \mu) = 0$ . In this way,

$$G_i^\mu(s_{i+}) = -\bar{G}_i(\mu^2). \quad (7)$$

In addition, we consider the prescription employed in Refs. [20,21], where a common scale  $\mu$  is chosen to be independent of the total angular momentum  $J$  [16,18], and equal to

$$\mu = \sqrt{\alpha(m_\pi^2 + M_{\Sigma_c}^2)}, \quad (8)$$

in the sectors of the  $\Lambda_c(2595)$  and  $\Lambda_c(2625)$  resonances. In the equation above,  $\alpha$  is a parameter that can be adjusted to data [20]. In what follows, we will refer to this scheme as  $SC\mu$  (subtraction at common scale).

In the second renormalization scheme, we make finite the UV divergent part of the loop function using a cutoff regulator  $\Lambda$  in momentum space, which leads to [39]

$$G_i^\Lambda(s_{i+}) = \frac{1}{4\pi^2} \frac{M_i}{m_i + M_i} \left( m_i \ln \frac{m_i}{\Lambda + \sqrt{\Lambda^2 + m_i^2}} + M_i \ln \frac{M_i}{\Lambda + \sqrt{\Lambda^2 + M_i^2}} \right). \quad (9)$$

Note that there are no cutoff effects in the finite  $\bar{G}_i(s)$ -loop function, as it would happen if the two-body propagator of Eq. (4) would have been directly calculated using the UV cutoff  $\Lambda$ .

If a common UV cutoff is used for all channels, both renormalization schemes are independent and will lead to different results. However, if one allows the freedom of using channel-dependent cutoffs, the subtraction at a common scale scheme,  $SC\mu$ , is recovered by choosing in each channel,  $\Lambda_i$  such that

$$G_i^{\Lambda_i}(s_{i+}) = -\bar{G}_i(\mu^2). \quad (10)$$

### C. Interplay between bare CQM and baryon-meson d.o.f.

Within the quark-model approach of Ref. [8], odd parity  $\Lambda^*$  states are obtained at 2628 and 2630 MeV for  $J = 1/2$  and  $3/2$ , respectively. The  $ldof$  are coupled to angular-momentum-parity-quantum numbers  $j_{ldof}^\pi = 1^-$  ( $\lambda$  mode) in both cases, which explains their approximate degeneracy. Higher excited states appear at 2.9 GeV ( $\rho$  mode), far from the  $\Lambda_c(2595)$  and  $\Lambda_c(2625)$  narrow resonances, and will not be considered in the present analysis. However, the low-lying  $\lambda$ -mode states, given their proximity to the  $\Lambda_c(2595)$  and  $\Lambda_c(2625)$ , might significantly influence the dynamics of the physical states. This seems to be specially truth for the  $\Lambda_c(2625)$ , since the prediction of Ref. [8] for its mass is only 2 MeV higher than the experimental one [ $(2628.11 \pm 0.19)$  MeV [10]].

Bare CQM states effects on the baryon-meson dynamics can be effectively considered by means of an energy dependent interaction [35,40,41]

$$V_{\text{ex}}^J(s) = 2\overset{\circ}{M}_{\text{CQM}} \frac{[V_{\text{CQM}}^J]^\dagger \cdot [V_{\text{CQM}}^J]}{s - (\overset{\circ}{M}_{\text{CQM}})^2},$$

$$V_{\text{CQM}}^{J=1/2} = \begin{pmatrix} \Sigma_c \pi & ND & ND^* \\ d_1 & \sqrt{3}c_1/2 & -c_1/2 \end{pmatrix}, \quad V_{\text{CQM}}^{J=3/2} = \begin{pmatrix} \Sigma_c^* \pi & ND^* \\ -d_1 & c_1 \end{pmatrix} \quad (11)$$

where  $d_1$  and  $c_1$  are undetermined dimensionless parameters that control the strength of the baryon-meson-CQM-state vertex. Note that  $[V_{\text{CQM}}^J]^\dagger \cdot [V_{\text{CQM}}^J]$  gives rise to  $3 \times 3$  and  $2 \times 2$  matrices in the  $J^P = 1/2^-$  and  $3/2^-$  sectors, respectively. The above interaction accounts for the contribution to baryon-meson scattering of the exchange of an intermediate odd parity CQM  $\lambda$ -mode state. It does not



obviously affect the  $j_{ldof}^\pi = 0^-$  subspace of the  $J^P = 1/2^-$  sector, and it is consistent with HQSS in the  $j_{ldof}^\pi = 1^-$  subspace of the  $J^P = 1/2^-$  and  $J^P = 3/2^-$  sectors, which are related by a spin rotation of the heavy quark. Actually, it is only thanks to HQSS that both sectors can be described by the same  $d_1$  and  $c_1$  LECs.<sup>2</sup>

Note that  $V_{\text{ex}}^J(s)$  introduces a pole in the baryon-meson tree-level amplitudes located at the bare mass value,  $\sqrt{s} = \overset{\circ}{M}_{\text{CQM}}$ . It should be interpreted as the mass of the CQM state in the limit of vanishing coupling to the baryon-meson-pairs ( $d_1, c_1 \rightarrow 0$ ), and therefore it is not an observable. The interaction with the baryon-meson cloud dresses the CQM state through loops, renormalizing its mass, and the dressed state might also acquire a finite width, when it is located above threshold. *A priori*,  $\overset{\circ}{M}_{\text{CQM}}$  is a free parameter of the present approach, and moreover it depends on the renormalization scheme [35]. This is because in the effective theory, the UV regulator is finite, and the difference between the bare and the physical resonance masses is a finite renormalization that depends on the adopted scheme. The value of the bare mass, which is thus a free parameter, can either be indirectly fitted to experimental observations, or obtained from schemes that ignore the coupling to baryon-meson pairs, such as some CQMs. In this latter case, the issue certainly would be to set the UV regulator to match the quark model and the baryon-meson scattering approaches [35]. For simplicity, and consistently with HQSS, we take a common bare mass for both  $J = 1/2$  and  $J = 3/2$ , which is fixed to the average of masses reported in the quark model of Ref. [8] ( $\overset{\circ}{M}_{\text{CQM}} = 2629$  MeV). We will explore different values of the renormalization scheme-dependent bare couplings  $d_1$  and  $c_1$  to elucidate the robustness of our results.

At energies far enough from  $\overset{\circ}{M}_{\text{CQM}}$ , the contribution of  $V_{\text{ex}}$  can be regarded as a small contact interaction that can be accounted for by means of a LEC. However, the exchange contribution becomes more important for energies approaching  $\overset{\circ}{M}_{\text{CQM}}$ , and it may not be safe to ignore its energy dependence. One might expect such a situation in the  $J = 3/2$  sector, where  $V_{\text{ex}}$  should provide a sizable attraction (repulsion) for energies slightly below (above)  $\overset{\circ}{M}_{\text{CQM}}$ , relevant in the dynamics of the  $\Lambda_c(2625)$ . We expect a less relevant role in the case of the  $\Lambda_c(2595)$ , since this resonance is located furthest from  $\overset{\circ}{M}_{\text{CQM}}$ .

<sup>2</sup>HQSS relations are straightforward when the  $\Sigma_c^{(*)}\pi$  and  $ND^{(*)}$  states are expressed in terms of the basis of well-defined *ldof* total angular momentum, where one can readily isolate the  $j_{ldof}^\pi = 1^-$  component of each baryon-meson pair [37].

## D. Riemann sheets, poles, and residues

Masses and widths of the dynamically generated resonances in each  $J^-$  sector are determined from the positions of the poles,  $\sqrt{s_R}$ , in the second Riemann sheet (SRS) of the corresponding baryon-meson scattering amplitudes, namely,  $\sqrt{s_R} = M_R - i\Gamma_R/2$ . In some cases, we also find real poles in the first Riemann sheet (FRS) which correspond to bound states. The different Riemann sheets are defined in terms of the multivalued function  $L(s)$ , introduced in Eq. (6), that is evaluated here as explained in Eq. (A13) of Ref. [38], and thus are labeled by  $\xi_1\xi_2\xi_3$  [ $\xi_1\xi_2$ ], with  $\xi_i = 0, 1$ , in the  $J = 1/2[3/2]$  sector. The SRS in the relevant fourth quadrant is obtained from the first quadrant FRS by continuity across each of the four unitarity cuts.

The coupling constants of each resonance to the various baryon-meson states are obtained from the residues at the pole by matching the amplitudes to the expression

$$T_{ij}^J(s) = \frac{g_i g_j}{\sqrt{s} - \sqrt{s_R}}, \quad (12)$$

for energy values  $s$  close to the pole, where the dimensionless couplings,  $g_i$ , turn out to be, in general, complex.

Note that when solving the BSE, we have neither considered the hadronic width of the  $D^*$  vector meson, nor those of the  $\Sigma_c$  and  $\Sigma_c^*$  baryons. The latter are of the order of 2 and 15 MeV, respectively, while the former one is just around 100 keV. They could be taken into account by convoluting the loop function  $G$  of these channels with the spectral function of the unstable particles, as done for instance in [42]. Because of the small widths of the  $D^*$  and  $\Sigma_c^{(*)}$  resonances, the effects on pole positions and couplings would not be relevant for the present discussion. Such effects only become relatively important when one deals with broad states, like the  $\rho$  meson or the  $\Delta$  baryon with widths of 150 or 120 MeV, respectively [42].

## E. The $\Lambda_c^*(1/2^-, 3/2) \rightarrow \Lambda_c(1/2^+) \pi\pi$ three-body decays through the $\pi\Sigma_c^{(*)}$ intermediate state

Isospin conservation forbids single pion transitions between the  $\Lambda_c^*$  and  $\Lambda_c$ , and hence the  $\Lambda_c^*(1/2^-, 3/2)$  decay into  $\Lambda_c$  and two pions. The decays proceed via an intermediate  $I = 1$  baryon state down to a  $\Lambda_c\pi$  pair. The relatively small masses of the  $\Lambda_c^*$ 's above  $\Lambda_c$  kinematically restrict the outgoing pion energies, making feasible a chiral derivative expansion [43]. There are two different final states,  $\Lambda_c^+\pi^-\pi^+$  and  $\Lambda_c^+\pi^0\pi^0$ , and we will consider here only the resonant term driven by the excitation of the  $\Sigma_c^{(*)}$  and its subsequent decay into  $\Lambda_c\pi$ , as shown in Fig. 1. This is by and large the dominant contribution to the  $\Lambda_c(2595)$  width, while it becomes significantly smaller for the  $\Lambda_c(2625)$  one, since the virtual  $\Sigma_c^*$  intermediate state is very much off shell [43,44]. Indeed the ARGUS Collaboration reported a ratio [45]  $R = \Gamma[\Lambda_c(2625) \rightarrow \Lambda_c^+\pi^+\pi^- (\text{non-resonant})] / \Gamma[\Lambda_c(2625) \rightarrow \Lambda_c^+\pi^+\pi^- (\text{total})] = 0.54 \pm 0.14$ .

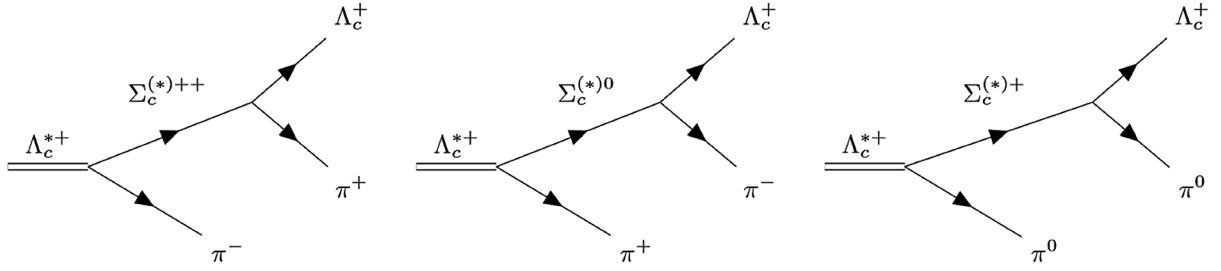


FIG. 1. Diagrams for  $\Lambda_c(2595)$  or  $\Lambda_c(2625)$  decay into  $\Lambda_c^+$  and two pions, mediated by the  $\Sigma_c$  or  $\Sigma_c^*$  resonances, respectively.

The  $\Lambda_c(2595)$  or  $\Lambda_c(2625)$  decay width into the charged-pions mode,<sup>3</sup> at lowest order in chiral perturbation theory and in the heavy mass limit, is given in the resonance rest frame (LAB) by [43]

$$\begin{aligned} \frac{d\Gamma_{\pi^-\pi^+}}{ds_{12}ds_{23}} &= \Gamma_0 \{ E_3^2 \vec{p}_2^2 |G_{\Sigma_c^{(*)}}(s_{12})|^2 + E_2^2 \vec{p}_3^2 |G_{\Sigma_c^{(*)}}(s_{13})|^2 + 2E_2 E_3 \text{Re}[G_{\Sigma_c^{(*)}}^*(s_{12}) G_{\Sigma_c^{(*)}}(s_{13})] \vec{p}_2 \cdot \vec{p}_3 \} \\ \Gamma_0 &= \frac{g_D^2 g_{R\Sigma_c^* \pi}^2 M_{\Lambda_c} M_{\Sigma_c^{(*)}}^2}{144 f_\pi^2 \pi^3 M_R^2 (M_R - M_{\Sigma_c^{(*)}})^2} \quad G_{\Sigma_c^{(*)}}(s) = \frac{1}{s - M_{\Sigma_c^{(*)}}^2 + i M_{\Sigma_c^{(*)}} \Gamma_{\Sigma_c^{(*)}}(s)} \\ \Gamma_{\Sigma_c^{(*)}}(s) &= \frac{g_D^2 M_{\Lambda_c}}{6\pi f_\pi^2 M_{\Sigma_c^{(*)}}} |\vec{p}_{\pi^{\Lambda_c \pi}}|^3, \quad |\vec{p}_{\pi^{\Lambda_c \pi}}| = \frac{\lambda^{\frac{1}{2}}(s, M_{\Lambda_c}^2, m_\pi^2)}{2\sqrt{s}}, \quad s_{13} = M_R^2 + 2m_\pi^2 + M_{\Lambda_c}^2 - s_{12} - s_{23} \\ E_3 &= \sqrt{m_\pi^2 + \vec{p}_3^2} = \frac{M_R^2 + m_\pi^2 - s_{12}}{2M_R}, \quad E_2 = \sqrt{m_\pi^2 + \vec{p}_2^2} = \frac{M_R^2 + m_\pi^2 - s_{13}}{2M_R}, \quad \vec{p}_2 \cdot \vec{p}_3 = E_2 E_3 + m_\pi^2 - s_{23}/2 \end{aligned} \quad (16)$$

with  $M_R$  the resonance mass,  $\lambda(x, y, z) = x^2 + y^2 + z^2 - 2xy - 2xz - 2yz$ . In addition,  $s_{12}$  (invariant mass square of  $\Lambda_c \pi^+$ ) varies between  $(M_{\Lambda_c} + m_\pi)^2$  and  $(M_R - m_\pi)^2$ , while the limits of  $s_{23}$  (invariant mass square of the  $\pi^+ \pi^-$  pair) are

$$s_{23}^{\text{max, min}} = (E_{\pi^+}^* + E_{\pi^-}^*)^2 - (p_{\pi^+}^* \mp p_{\pi^-}^*)^2, \quad E_{\pi^+}^* = \frac{s_{12} + m_\pi^2 - M_{\Lambda_c}^2}{2\sqrt{s_{12}}}, \quad E_{\pi^-}^* = \frac{M_R^2 - m_\pi^2 - s_{12}}{2\sqrt{s_{12}}} \quad (17)$$

with  $p_{\pi^\pm}^{*2} = E_{\pi^\pm}^{*2} - m_\pi^2$ . The expression of Eq. (16) corresponds to the square of the sum of amplitudes associated to the first two diagrams of Fig. 1. In addition  $g_D/f_\pi = 0.0074 \text{ MeV}^{-1}$ , which leads to  $\Gamma[\Sigma_c \rightarrow \Lambda_c \pi] = 1.9 \text{ MeV}$  and  $\Gamma[\Sigma_c^* \rightarrow \Lambda_c \pi] = 14.4 \text{ MeV}$ , and we take the dimensionless coupling  $g_{R\Sigma_c^* \pi}$  from the residue at the resonance pole [Eq. (12)] of the  $\Sigma_c^{(*)} \pi$  channel ( $S$  wave) that we choose to be real, by an appropriate redefinition of the overall phases of the meson and baryon fields.

<sup>3</sup>The  $\Lambda(2595)$  and  $\Lambda(2625)$  amplitudes read

$$T_{\pi^-\pi^+}^{J=1/2} = -\frac{g_D g_{R\Sigma_c \pi}}{3f_\pi} \frac{2M_{\Sigma_c}}{(M_R - M_{\Sigma_c})} \bar{u}_{\Lambda_c} \left\{ (v p_{\pi^-}) G_{\Sigma_c}(s_{12}) (\not{p}_{\pi^+} + v p_{\pi^+}) \gamma_5 \frac{1 + \not{v}}{2} + (v p_{\pi^+}) G_{\Sigma_c}(s_{13}) (\not{p}_{\pi^-} + v p_{\pi^-}) \gamma_5 \frac{1 + \not{v}}{2} \right\} u_R \quad (13)$$

$$T_{\pi^-\pi^+}^{J=3/2} = \frac{g_D g_{R\Sigma_c \pi}}{3f_\pi} \frac{2M_{\Sigma_c}}{(M_R - M_{\Sigma_c})} [(v p_{\pi^-}) G_{\Sigma_c}(s_{12}) p_{\pi^+}^\mu + (v p_{\pi^+}) G_{\Sigma_c}(s_{13}) p_{\pi^-}^\mu] \bar{u}_{\Lambda_c} P_{\mu\nu}(v) u_R^\nu \quad (14)$$

where  $v$  is the common velocity of all involved charmed hadrons, which remains unaltered in the heavy quark limit. It satisfies  $v^2 = 1$  and  $\not{v} u_R^{(\nu)} = u_R^{(\nu)}$  and  $\not{v} u_{\Lambda_c} = u_{\Lambda_c}$ , with  $u$  and  $u^\nu$  mass dimensions of the Dirac and Rarita-Schwinger spinors, respectively. The spin-3/2 projector is

$$P^{\mu\nu}(v) = \left( -g^{\mu\nu} + v^\mu v^\nu + \frac{1}{3} (\gamma^\mu + v^\mu) (\gamma^\nu - v^\nu) \right) \frac{1 + \not{v}}{2} \quad (15)$$

with metric  $(+, -, -, -)$ , and the sum over fermion polarizations is given by  $u\bar{u} = 2M(1 + \not{v})/2$  and  $u^\mu \bar{u}^\nu = 2MP^{\mu\nu}$ .

The processes occur so close to threshold, especially the  $\Lambda_c(2595)$  decay, that the available phase space might depend significantly on the small isospin-violating mass differences between members of the pion and  $\Sigma_c^{(*)}$  multiplets.<sup>4</sup> We have used  $m_\pi = m_{\pi^\pm}$ ,  $M_{\Sigma_c^{(*)}} = (M_{\Sigma_c^{+(*)}} + M_{\Sigma_c^{0(*)}})/2$ ,  $M_{\Lambda_c(2595)} = 2592.25$  MeV and  $M_{\Lambda_c(2625)} = 2628.11$  MeV. The errors on the masses of the  $\Lambda_c^*$  resonances quoted in the review of particle properties [10] are 0.28 and 0.19 MeV, respectively, and turn out to be relevant only for the  $\Lambda_c(2595)$  width, but even in that case, it induces variations of the order of 1%.

The rates for the neutral-pions channel can be obtained by adding a symmetry factor 1/2 to avoid double counting the two identical bosons in the final state and using  $m_\pi = m_{\pi^0}$ ,  $M_{\Sigma_c^{(*)}} = M_{\Sigma_c^{+(*).}}$

Adding the contribution of neutral and charged-pion modes, we find that the  $\Sigma_c^{(*)}$ -resonant contribution to the  $\Lambda_c(2595)$  and  $\Lambda_c(2625)$  decays into  $\Lambda_c^+$  and two pions are

$$\begin{aligned}\Gamma[\Lambda_c(2595) \rightarrow \Lambda_c \pi \pi] &= 1.84 \times g_{\Lambda_c(2595)\Sigma_c \pi}^2 [\text{MeV}], \\ \Gamma[\Lambda_c(2625) \rightarrow \Lambda_c \pi \pi] &= 0.27 \times g_{\Lambda_c(2625)\Sigma_c^* \pi}^2 [\text{MeV}]\end{aligned}\quad (18)$$

with the  $\pi^0\pi^0$  channel being the 81.5% and 45.0% of the total for the  $\Lambda_c(2595)$  and  $\Lambda_c(2625)$  partial widths, respectively. In the exact isospin limit, the two-neutral-pions partial width is a factor of 2 smaller than the  $\pi^+\pi^-$  one. The experimental width of the  $\Lambda_c(2595)$  is  $2.6 \pm 0.6$  MeV (nearly 100% saturated by the two  $\Lambda_c \pi \pi$  modes), while there exists an upper bound of 0.97 MeV for the  $\Lambda_c(2625)$  [10]. Hence, the experimental  $\Gamma[\Lambda_c(2595)]$  provides a direct measurement of the  $S$ -wave coupling constant  $g_{\Lambda_c(2595)\Sigma_c \pi}^2$ , assuming that a possible  $D$ -wave contribution is negligible [46]. The bound on  $\Gamma[\Lambda_c(2625)]$ , on the other hand, puts upper limits on the coupling in  $S$  wave of this resonance to the  $\Sigma_c^* \pi$  pair, but one should bear in mind that in this case, the resonant contribution does not saturate the decay width.

The interference term in Eq. (16) for the charged mode, and the equivalent one in the case of  $\pi^0\pi^0$ , gives a small contribution to the integrated width. In particular for the  $\Lambda_c(2595)$ , it is of the order of  $-1\%$  and  $-0.2\%$  for the  $\pi^+\pi^-$  and  $\pi^0\pi^0$  channels, respectively. For the  $\Lambda_c(2625)$ , it becomes larger around  $-5\%$  and  $-4\%$ , respectively, but it is still quite small. This can be easily understood by changing the  $s_{12}$  and  $s_{23}$  integration variables to  $E_3$  and  $\cos\theta_{23}$ , with  $\theta_{23}$  the angle formed by the two pions in the resonance rest frame. The energy  $E_2$  (or equivalently  $s_{13}$ ) depends on  $\cos\theta_{23}$  through the conservation of energy equation,  $M_R = E_3(\vec{p}_3) + E_2(\vec{p}_2) + E_{\Lambda_c}(\vec{p}_2 + \vec{p}_3)$ . In the

infinite charm limit, the recoiling  $\Lambda_c$  baryon carries off momentum but not kinetic energy, and hence the approximation [43]

$$E_2 \sim M_R - M_{\Lambda_c} - E_3 \quad (19)$$

turns out to be quite accurate, especially for the  $\Lambda_c(2595)$  where the energy released by the decaying resonance is very small. Within this approximation, the only dependence of the differential decay rate on  $\cos\theta_{23}$  comes from the scalar product  $\vec{p}_2 \cdot \vec{p}_3$  in the interference term, which would vanish in the integrated width, since  $\cos\theta_{23}$  covers almost totally the  $[-1, 1]$  range for all  $E_3$  allowed values. Indeed, we recover Eq. (3.5), up to a factor 1/2, of Ref. [43] from the expression of Eq. (16) by neglecting the interference term and adopting the approximation of Eq. (19), using that  $ds_{12} = 2M_R dE_3$  and taking into account that the integration over  $ds_{23}$  gives  $4p_{\pi^+}^* p_{\pi^-}^* \sim 4\sqrt{E_3^2 - m_\pi^2} \sqrt{E_2^2 - m_\pi^2}$ , approximating in the propagators  $(s_{12(13)} - M_{\Sigma_c^{(*)}}^2)$  by  $2M_{\Sigma_c^{(*)}}(M_R - E_{3(2)} - M_{\Sigma_c^{(*)}})$ , and finally identifying  $g_D^2 = h_1^2/2$  and  $g_{R\Sigma_c^* \pi}^2 = 3h_2^2(M_R - M_{\Sigma_c^{(*)}})^2/(2f_\pi^2)$ , with  $h_{1,2}$  used in Ref. [43]. The factor 1/2 introduced in this latter work does not hold for the  $\pi^+\pi^-$  decay mode, though should be included for the neutral mode.<sup>5</sup>

We would like to mention that three-body  $\Lambda_c(2595) \rightarrow \Lambda_c \pi \pi$  decay rate can be approximated by using the narrow width approximation of the  $\Sigma_c^{(*)}$  propagators,

$$|G_{\Sigma_c}(s)|^2 \sim \frac{\pi}{M_{\Sigma_c} \Gamma_{\Sigma_c}(s)} \delta(s - M_{\Sigma_c}^2) = \frac{6\pi f_\pi^2}{M_{\Lambda_c} |\vec{p}_\pi^{\Lambda_c \pi}|^3} \delta(s - M_{\Sigma_c}^2) \quad (20)$$

which leads to

$$\begin{aligned}\Gamma_{\pi^-\pi^+} &\sim (\Gamma_{\Lambda_c(2595) \rightarrow \Sigma_c^{++} \pi^-} + \Gamma_{\Lambda_c(2595) \rightarrow \Sigma_c^0 \pi^+}), \\ \Gamma_{\pi^0\pi^0} &\sim \Gamma_{\Lambda_c(2595) \rightarrow \Sigma_c^+ \pi^0}\end{aligned}\quad (21)$$

$$\begin{aligned}\Gamma_{\Lambda_c(2595) \rightarrow \Sigma_c^a \pi^b} &= \frac{g_{\Lambda_c(2595)\Sigma_c \pi}^2}{6\pi} \frac{M_{\Sigma_c^a}}{M_{\Lambda_c(2595)}} |\vec{p}_\pi|, \\ |\vec{p}_\pi| &= \frac{\lambda^{\frac{1}{2}}(M_{\Lambda_c(2595)}^2, M_{\Sigma_c^a}^2, m_{\pi^b}^2)}{2M_{\Lambda_c(2595)}}\end{aligned}\quad (22)$$

for the charge combinations  $(a, b) = (++, -)$ ,  $(0, +)$ , and  $(+, 0)$ , which correspond to the square of the amplitudes of each of the three diagrams depicted in Fig. 1. To obtain Eq. (21) from Eq. (16), using the approximation of Eq. (20), we have neglected the interference contributions,

<sup>4</sup>For the same reason, we have here explicitly included the energy dependent widths of the intermediate  $\Sigma_c$  and  $\Sigma_c^*$  resonances [10].

<sup>5</sup>Note, however, that the expression for the  $\Lambda_c \pi^0 \pi^0$  partial width used by the CDF Collaboration in Ref. [46] is wrong by a factor of 2. The 1/2 in Eq. (13) for the amplitude in that reference should be replaced by  $1/\sqrt{2}$ .

have approximated the LAB energy of the nonresonant pion and the momentum of the resonant one by  $(M_{\Lambda_c(2595)} - M_{\Sigma_c})$  and  $|\vec{p}_\pi|$ , respectively, and, in addition, we have made use of the fact that the momentum of the nonresonant pion in the  $\Sigma_c$  rest frame is  $M_{\Lambda_c(2595)}|\vec{p}_\pi|/M_{\Sigma_c}$ . The two-body  $S$ -wave-widths limit of Eq. (21) works well when the intermediate  $\Sigma_c$  is nearly on shell. The value used here for  $M_{\Lambda_c(2595)}$  is 1.2 (4.6) MeV below (above) the  $\Sigma_c^{++0} m_{\pi^\mp}$  ( $\Sigma_c^+ m_{\pi^0}$ ) threshold. We find that  $\Gamma_{\pi^0\pi^0}$  and  $\Gamma_{\Lambda_c(2595)\rightarrow\Sigma_c^+\pi^0}$  differ only in  $0.19 g_{\Lambda_c(2595)\Sigma_c\pi}^2$  [MeV], this is to say, the latter width is just 2.5% greater than the former one. The  $\Sigma_c^{++}$  and  $\Sigma_c^0$  cannot be put on shell for this mass of the  $\Lambda_c(2595)$ , but clearly the differential decay width of Eq. (16) is strongly dominated by the contribution of two well-separated peaks that correspond to the first two mechanisms shown in Fig. 1 [43].

Finally, we should acknowledge that we have neither considered direct two pion emission processes mediated by heavier  $\Sigma_c^{(*)}$ - resonances, nor  $\pi\pi$  or  $\pi\Lambda_c$  final state-interactions (FSI) effects. In the case of the  $\Lambda_c(2595)$ , the decay is dominated by the intermediate  $\Sigma_c(2455)$  mechanism [10]. Indeed, the ARGUS Collaboration reported a value of  $0.66_{-0.16}^{+0.13} \pm 0.07$  for the ratio of the resonant contribution to width and total width [47], while the results of the E687 Collaboration are consistent with this ratio being 100% [48]. Other mechanisms are then expected to be significantly smaller. We should bear in mind that we only use the three body decays of the  $\Lambda_c(2595)$  and  $\Lambda_c(2625)$  to limit the acceptable values of the couplings of these resonances to the  $\Sigma_c^{(*)}\pi$  pairs, and thus considering only the intermediate  $\Sigma_c(2455)$  contribution is sufficiently accurate for our purposes. On the other hand, pions are produced almost at threshold and hence one should expect small effects from their FSI. The  $\pi\Lambda_c$  FSI are, however, large, and are dominated by the production of the  $\Sigma_c(2455)$ , whose effects are explicitly taken into account thanks to the complex propagator of this intermediate resonance. For the  $\Lambda_c(2625)$  case, contact two pion emission processes can be more relevant. However, the strongest bound for  $g_{\Lambda_c(2625)\Sigma_c^+\pi}^2$  comes from the  $\Sigma_c^*(2520)$  resonant contribution measured by the ARGUS Collaboration [45], which is precisely what we compute here using the mechanisms depicted in Fig. 1.

### III. RESULTS AND DISCUSSION

#### A. $SU(6)_{\text{lsf}} \times \text{HQSS}$ hadron molecules: Dependence on the renormalization scheme

First, we present in Fig. 2 the dynamically generated resonances (poles in the SRS of the amplitudes) that are obtained, when the effects produced by the exchange of CQM bare states are neglected. We show both the  $J = 1/2$  and  $J = 3/2$  sectors, and consider the two renormalization

schemes introduced in Sec. II B. The numerical positions of the poles and residues are given in the first row of Tables I and II.

The  $SC\mu$  results found here, working with the reduced  $ND^{(*)} - \Sigma_c^{(*)}\pi$  coupled-channels space, reproduce reasonably well the most important features reported in the original works of Refs. [20,21]. Indeed, we choose  $\alpha = 0.95$  to better account for some of the effects produced by the channels that have not been considered in the current approach. We see that a narrow  $J^P = 1/2^- \Lambda_{c(n)}^{0-}(2595)$  resonance ( $\Gamma \sim 2$  MeV) is produced. This is mostly generated from the extended  $WT ND - ND^*$  coupled-channels dynamics in the  $j_{\text{dof}}^\pi = 0^-$  subspace. This state has a small coupling to the  $(j_{\text{dof}}^\pi = 1^-)\Sigma_c\pi$  channel which, in addition to the proximity to the open threshold, explains its small width. There appears a second  $J^P = 1/2^-$  pole [ $\Lambda_{c(b)}^{1-}(2595)$ ] in the 2.6 GeV region. Although it is placed relatively close to the  $\Sigma_c\pi$  threshold, this resonance is broad ( $\Gamma \sim 75$  MeV) because of its sizable coupling to the latter open channel. Nevertheless, as seen in Fig. 2, this second wide state will not produce visible effects on the baryon-meson  $S$ -wave cross sections, since its possible impact for real values of  $s$  will be shadowed by the narrow  $\Lambda_{c(n)}^{0-}$  that is located at a similar mass and much closer to the scattering line. Thus, this double pattern structure would be difficult to be confirmed experimentally, and it will not certainly show up in the  $\Lambda_c\pi\pi$  spectrum, where the evidence of the  $\Lambda_c(2595)$  has been reported [46,47,49]. However, it has been argued that exclusive semileptonic  $\Lambda_b$  ground-state decays in excited charmed  $\Lambda_c^*$  baryons could unravel the two  $\Lambda_c(2595)$  states [37,50], if they exist.

In the  $J^P = 3/2^-$  sector, we find a resonance that clearly is the HQSS partner of the broad  $J^P = 1/2^- \Lambda_{c(b)}^{1-}(2595)$  state, with quantum numbers  $1^-$  for  $j_{\text{dof}}^\pi$ . It is located above the  $\Sigma_c^*\pi$  threshold, with a width of around 55 MeV. Furthermore, the coupling of this  $J^P = 3/2^-$  pole to the  $\Sigma_c^*\pi$  channel is essentially identical to that of the  $\Lambda_{c(b)}^{1-}(2595)$  to  $\Sigma_c\pi$ . This  $J^P = 3/2^-$  isoscalar resonance might be identified with the  $D$  wave  $\Lambda_c(2625)$ , although its mass and width significantly differ from those of the physical state. In Refs. [20,21], it is argued that a change in the renormalization subtraction constant could move the resonance down by 40 MeV to the nominal position of the physical state, and that, in addition, this change of the mass would considerably reduce the width, since the state might even become bound below the  $\Sigma_c^*\pi$  threshold. Thus, within the  $SU(6)_{\text{lsf}} \times SU(2)_{\text{HQSS}}$  model, the  $\Lambda_c(2625)$  would turn out to be the HQSS partner of the second broad  $\Lambda_{c(b)}^{1-}(2595)$  pole instead of the narrow  $\Lambda_{c(n)}^{0-}(2595)$  resonance.<sup>6</sup> This is

<sup>6</sup>A more detailed discussion, incorporating some elements of group theory, can be found in [21] and in Sec. 2.2.1 of Ref. [37].



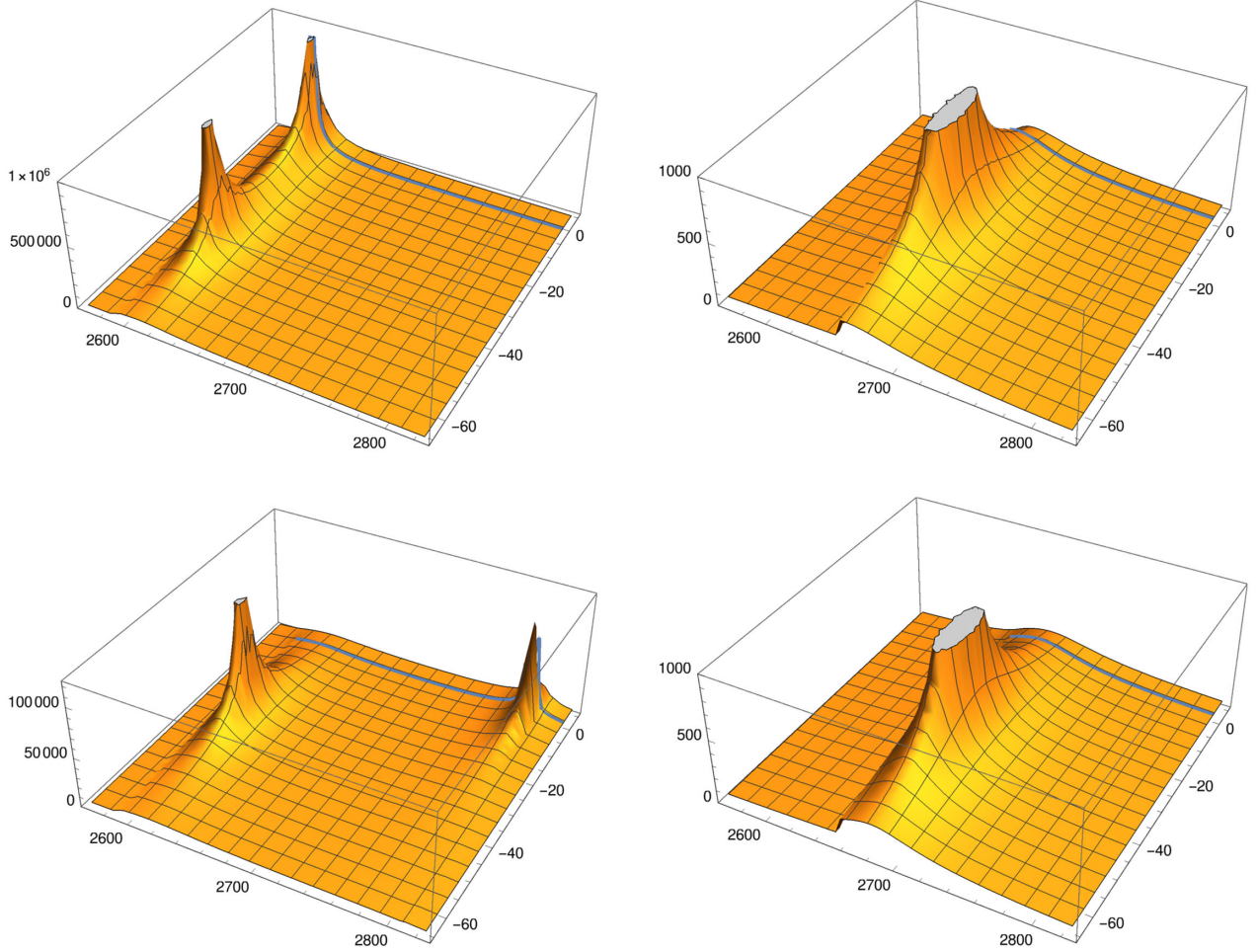


FIG. 2. Absolute value of the determinant of the  $T$  matrix (AVD- $T$ ) in the  $J^P = 1/2^-$  (left) and  $J^P = 3/2^-$  (right) sectors using two UV renormalization schemes:  $SC\mu$  with  $\alpha = 0.95$  and a cutoff of 650 MeV in the top and bottom panels, respectively. We display the AVD- $T$  for both the FRS [ $\text{Im}(E) > 0$ ] and the SRS [ $\text{Im}(E) < 0$ ] [fm] of the unitarized amplitudes as a function of the complex energy  $E$  [MeV]. We also show the scattering line (blue solid curve) in all the cases. Bare CQM exchange interactions are set to zero [ $d_1 = c_1 = 0$  in Eq. (11)]. In the  $z$  axis we have AVD- $T$ , in the  $x$  axis we have  $\text{Re}(E)$ , and in the  $y$  axis we have  $\text{Im}(E)$ .

in sharp contrast to the predictions of the CQMs, where there is no second 2595 pole, and the  $\Lambda_c(2625)$  and the narrow  $\Lambda_c(2595)$  are HQSS siblings, produced by a  $\lambda$ -mode excitation of the ground  $1/2^+$   $\Lambda_c$  baryon.

The  $SC\mu$ -renormalization scheme plays an important role in enhancing the influence of the  $ND^*$  channel in the dynamics of the narrow  $\Lambda_{c(n)}^{0-}(2595)$  state. Indeed, this scheme also produces a reduction in the mass of the

TABLE I. Properties of the CQM and molecular  $J^P = 3/2^-$  poles for different renormalization schemes and values of the  $d_1$  and  $c_1$  LECs, which determine the interplay between CQM and baryon-meson pair degrees of freedom. The angular-momentum-parity quantum numbers of the  $ldof$  are always  $1^-$ , and masses and widths are given in MeV units.

$d_1$	$c_1$	$\Lambda = 650$ MeV				$SC\mu$ ( $\alpha = 0.95$ )			
		$M - i\Gamma/2$	Type	$ g_{\Sigma_c^* \pi} $	$ g_{ND^*} $	$M - i\Gamma/2$	Type	$ g_{\Sigma_c^* \pi} $	$ g_{ND^*} $
0	0	(2680.4 - $i33.0$ )	$1^-$	2.0	2.5	(2662.6 - $i27.2$ )	$1^-$	2.3	2.4
-0.8	0	(2704.0 - $i31.5$ )	$1^-$	1.7	2.2	(2688.8 - $i28.4$ )	$1^-$	1.8	1.9
-0.8	0	2615.8	CQM	1.0	0.6	2617.5	CQM	1.1	0.5
-0.8	-1	(2706.8 - $i30.2$ )	$1^-$	1.7	2.6	(2681.1 - $i27.0$ )	$1^-$	1.8	2.4
-0.8	-1	2614.9	CQM	1.1	0.2	2617.7	CQM	1.0	0.5
-0.8	1	(2701.4 - $i32.4$ )	$1^-$	1.8	1.8	(2695.5 - $i30.6$ )	$1^-$	1.8	1.5
-0.8	1	2620.9	CQM	0.9	1.5	2612.9	CQM	1.2	1.4

TABLE II. Properties of the CQM and molecular  $J^P = 1/2^-$  poles for different renormalization schemes and values of the  $d_1$  and  $c_1$  LECs, which determine the interplay between CQM and baryon-meson pair degrees of freedom. Molecular states are labeled according to their dominant  $ldof$  configuration,  $0^-$  or  $1^-$ , and masses and widths are given in MeV units.

$d_1$	$c_1$	$\Lambda = 650$ MeV					$SC\mu$ ( $\alpha = 0.95$ )				
		$M - i\Gamma/2$	Type	$ g_{\Sigma_c\pi} $	$ g_{ND} $	$ g_{ND^*} $	$M - i\Gamma/2$	Type	$ g_{\Sigma_c\pi} $	$ g_{ND} $	$ g_{ND^*} $
0	0	(2609.9 - $i28.8$ )	$1^-$	2.0	2.3	0.7	(2608.9 - $i38.6$ )	$1^-$	2.3	2.0	1.9
0	0	(2798.7 - $i2.0$ )	$0^-$	0.3	1.8	4.1	(2610.2 - $i1.2$ )	$0^-$	0.5	3.9	6.2
-0.8	0	2590.0	$1^-$	1.1	1.0	0.3	2591.1 <sup>a</sup>	$1^-$	1.3	1.5	0.5
-0.8	0	(2799.0 - $i2.2$ )	$0^-$	0.3	1.8	4.1	(2611.6 - $i0.4$ )	$0^-$	0.3	3.5	6.2
-0.8	0	(2659.1 - $i17.3$ )	CQM	1.3	1.6	0.3	(2652.8 - $i22.2$ )	CQM	1.5	0.8	1.7
-0.8	-1	2589.3	$1^-$	1.2	0.5	0.2	(2589.4 - $i8, 6$ ) <sup>a</sup>	$1^-$	2.6	1.7	0.7
-0.8	-1	(2800.7 - $i2.3$ )	$0^-$	0.3	1.7	4.1	(2610.1 - $i0.0$ )	$0^-$	0.0	3.8	5.9
-0.8	-1	(2657.2 - $i15.8$ )	CQM	1.2	2.3	0.5	(2642.3 - $i19.4$ )	CQM	1.5	1.1	2.5
-0.8	1	2591.0	$1^-$	0.9	1.2	0.4	2590.3	$1^-$	1.1	1.7	0.5
-0.8	1	(2798.8 - $i1.9$ )	$0^-$	0.3	1.8	4.1	(2612.6 - $i0.7$ )	$0^-$	0.4	3.2	6.3
-0.8	1	(2660.0 - $i18.9$ )	CQM	1.3	1.1	0.2	(2659.6 - $i26.8$ )	CQM	1.6	0.7	1.2

<sup>a</sup>Virtual state placed in the 100 sheet below the  $\Sigma_c\pi$  threshold.

resonance of around 200 MeV, which thus appears in the region of 2.6 GeV, instead of in the vicinity of the  $ND$  threshold. Indeed, we see also in Fig. 2 and Table II that if the UV behavior of the amplitudes is renormalized by means of a common momentum cutoff of 650 MeV [Eq. (9)], the position of the  $j_{ldof}^\pi = 0^-$  pole in the  $J^P = 1/2^-$  sector moves up drastically, and it now appears at 2.8 GeV with few chances to be identified with the physical  $\Lambda_c(2595)$  state. It is still narrow, because HQSS prevents its coupling to  $\Sigma_c\pi$  to become large. However, the main features of the broad  $J^P = 3/2^-$  resonance and the  $j_{ldof}^\pi = 1^-$  one in the  $J = 1/2$  sector are not much affected by the change of renormalization scheme. The mass position of the latter resonance can be moved down to the vicinity of the  $\Sigma_c\pi$  threshold using cutoffs of the order of 750 MeV, which is still reasonable. At the same time, its width also decreases since the available phase space for the decay becomes smaller. However, to obtain masses for the  $3/2$  state of around 2625 MeV, significantly larger cutoffs of the order of 1200 MeV are needed. This might hint at the existence of some further contributions to those induced for the baryon-meson unitarity loops, and that are effectively accounted for in the somehow unnatural UV regulator. In this context, we will discuss in the next subsection effects produced by CQM d.o.f. In addition, the coupling  $|g_{\Sigma_c\pi}|$  would take values of around 1.6 leading to  $\Gamma[\Lambda_c(2625) \rightarrow \Lambda_c\pi\pi] \sim 0.7$  MeV from Eq. (18), 30% below the upper bound on the total width of the resonance. However, taking into account that the  $\Sigma_c^*$  resonant contribution measured by the ARGUS Collaboration is  $(46 \pm 14)\%$  [45] of the total, we find that 0.7 MeV is around two sigmas above the inferred upper bound for the resonant mechanism. Note that using Eq. (18), the upper bound on the  $\Sigma_c^*$ -resonant contribution to the  $\Lambda_c(2625)$  width leads to

$$|g_{\Sigma_c\pi}| < 1.3 \pm 0.2. \quad (23)$$

We end this discussion by studying the relation between the cutoff and  $SC\mu$  UV renormalization schemes. Results obtained in  $SC\mu$  are recovered by using appropriate channel-dependent cutoffs as detailed in Eq. (10). These are 459, 544, 905, and 1044 MeV for  $\pi\Sigma_c$ ,  $\pi\Sigma_c^*$ ,  $ND$ , and  $ND^*$ , respectively. We see that the cutoff for  $ND^*$  is large and it enhances the importance of this channel in the dynamics of the narrow  $\Lambda_{c(n)}^{0-}(2595)$  resonance found in the  $SC\mu$  scheme.

## B. CQM and baryon-meson d.o.f.

As mentioned in Sec. II C, the quark model of Ref. [8] predicts a ( $J^P = 1/2^-, 3/2^-$ ) HQSS doublet of states, almost degenerate and with  $\tilde{M}_{CQM} \sim 2629$  MeV. Though with some precautions, because the CQM bare mass is not an observable and the matching procedure between the quark model and the effective hadron theory is not well defined, it seems natural to think that the bare CQM states should have a important influence in the dynamics of the  $\Lambda_c(2595)$  and  $\Lambda_c(2625)$  resonances, which are located so close. Indeed, the baryon-meson interactions of Eq. (11), driven by the exchange of the CQM state, have a strong energy dependence close to  $\tilde{M}_{CQM} \sim 2629$  that might be difficult to accommodate by just modifying the real part of the unitarity loops. The LECs  $c_1$  and  $d_1$ , that control the interplay between bare CQM and baryon-meson d.o.f., are unknown. They are also renormalization scheme dependent, and once the scheme is fixed, they should be inferred from data. The hope is that in this way, some theoretical predictions could become renormalization independent, at least in some energy window around the experimental inputs.

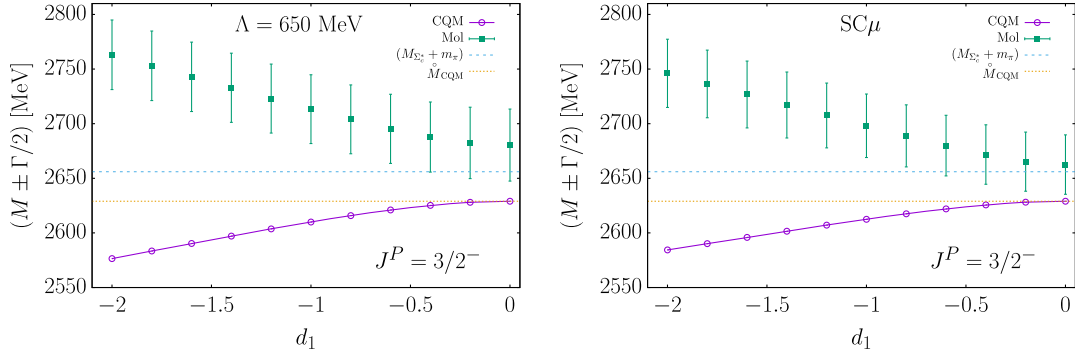


FIG. 3. Dependence of the  $J^P = 3/2^-$  CQM and molecular pole positions as a function of the LEC  $d_1$ , for  $c_1 = 0$ . We show results for both, the cutoff and  $SC\mu$  ( $\alpha = 0.95$ ) renormalization schemes, and the values of the bare CQM mass and the  $\Sigma_c^*\pi$  threshold energy.

### 1. The $\Lambda_c(2625)$

First we pay attention to the  $J^P = 3/2^-$  sector. In Figs. 3, 4, and 5, we show results obtained using  $SC\mu$  ( $\alpha = 0.95$ ) or a common UV cutoff of 650 MeV for different CQM and baryon-meson couplings. In principle, one expects that  $d_1$  should be more relevant than  $c_1$  because the  $\Sigma_c^*\pi$  threshold is closer to  $\overset{\circ}{M}_{CQM}$  than the  $ND^*$  one. Thus, in a first stage we set  $c_1$  to zero and start varying  $d_1$ . Results are depicted in Fig. 3 (note that in this situation, the irreducible amplitudes depend on  $d_1^2$ ). There are now two poles in both renormalization schemes. The lightest one is located below the  $\Sigma_c^*\pi$  threshold and it tends to  $\overset{\circ}{M}_{CQM}$  when  $d_1 \rightarrow 0$ . Its coupling to  $\Sigma_c^*\pi$ ,  $|g_{\Sigma_c^*\pi}|$ , grows from zero, when  $d_1 = 0$ , to values of around 1.8 or 1.9, when  $d_1 = -2$ , for the UV cutoff or  $SC\mu$  renormalization schemes, respectively. The upper bound of Eq. (23) is not satisfied above  $|d_1| > 1.2(1.0)$  for the  $\Lambda = 650$  MeV ( $SC\mu$ ) scheme.

On the other hand, the second pole, located at higher masses, is a broad resonance, with a width of around 60 MeV and little sensitivity to  $d_1$ . Indeed, as can be seen in the figure, the width varies less than 2 (8) MeV in the UV cutoff ( $SC\mu$ ) scheme, when  $d_1$  changes from 0 to  $-2$ . The

mass of this second resonance is more affected by  $d_1$ , and gets bigger when  $d_1^2$  increases, since the CQM exchange interaction is repulsive for energies above  $\overset{\circ}{M}_{CQM}$ . The pole matches the  $SU(6)_{\text{lf}} \times \text{HQSS}$  molecular one discussed in Sec. III A, when the coupling between CQM and baryon-meson d.o.f. is switched off.

Within the nonrelativistic CQM used in Ref. [12], the LEC  $d_1$  is predicted to be  $-0.8$ . With all cautions, already mentioned, about the matching between quark models and hadron-hadron based images of the problem, and the dependence on the renormalization procedure, we will fix  $d_1$  to the latter value, and study the dependence of the previous results on  $c_1$ . We let this latter parameter vary in the range  $-3$  to  $2$  in Fig. 4, where the  $|g_{\Sigma_c^*\pi}|$  and  $|g_{ND^*}|$  couplings, the mass and  $\Sigma_c^*\pi$ - molecular probability of the  $J^P = 3/2^-$  dressed CQM pole are shown as a function of  $c_1$ . The molecular probability is defined through Weinberg's compositeness rule [51,52], generalized for the coupled-channels BSE formalism in Refs. [53,54],

$$P_{\Sigma_c^*\pi} = -g_{\Sigma_c^*\pi}^2 \frac{\partial G_{\Sigma_c^*\pi}(\sqrt{s})}{\partial \sqrt{s}} \Big|_{\sqrt{s}=\sqrt{s_R}}. \quad (24)$$

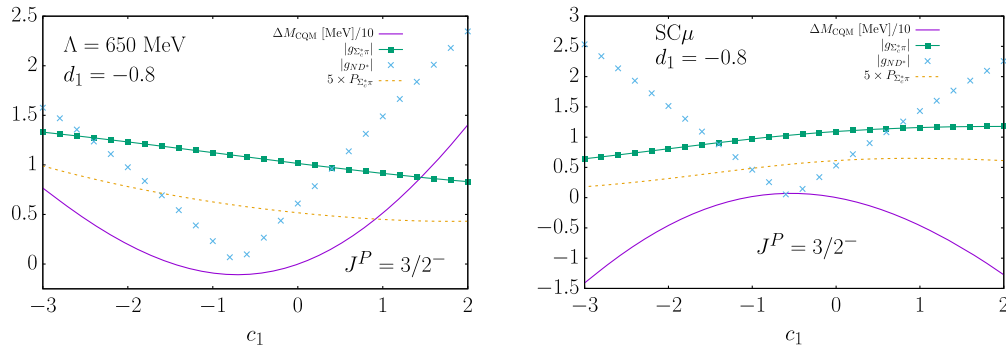


FIG. 4. Dependence of the couplings, mass and  $\Sigma_c^*\pi$ - molecular probability of the  $J^P = 3/2^-$  dressed CQM pole as a function of the LEC  $c_1$ , for  $d_1 = -0.8$ . We show results for both, the cutoff and  $SC\mu$  ( $\alpha = 0.95$ ) renormalization schemes. In addition,  $\Delta M_{CQM} = [M_{CQM}(d_1) - M_{CQM}(d_1 = -0.8)]$ , with  $M_{CQM}(d_1 = -0.8) = 2615.81$  and  $2617.49$  MeV for the left and right panels, respectively.



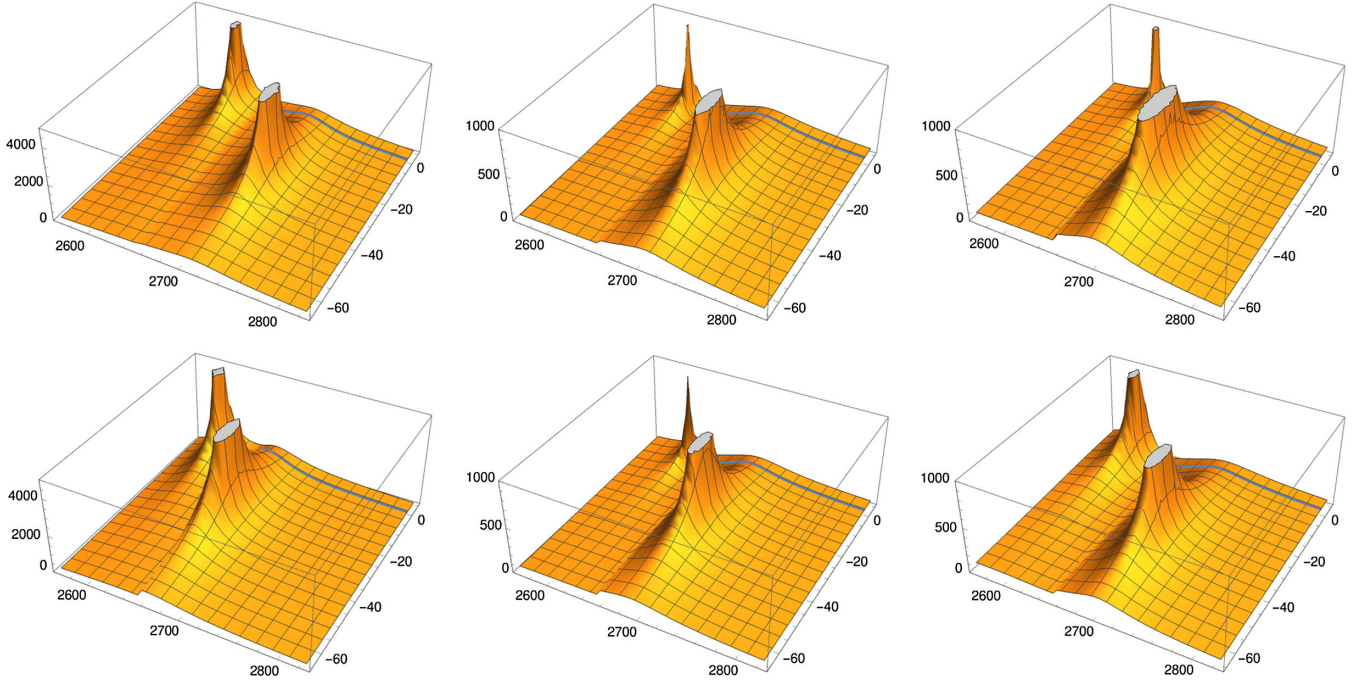


FIG. 5. AVD- $T$  in the  $J^P = 3/2^-$  sector using two UV renormalization schemes:  $SC\mu$  ( $\alpha = 0.95$ ) and a cutoff of 650 MeV in the bottom and top panels, respectively, for different CQM and baryon-meson pair couplings (from left to right):  $(c_1 = -3, d_1 = -0.8)$ ,  $(c_1 = 0, d_1 = -0.8)$ , and  $(c_1 = 2, d_1 = -0.8)$ . We display the AVD- $T$  for both the FRS [ $\text{Im}(E) > 0$ ] and the SRS [ $\text{Im}(E) < 0$ ] [fm] of the unitarized amplitudes as a function of the complex energy  $E$  [MeV]. We also show the scattering line (blue solid curve) in all the cases. Axes are defined as in Fig. 2.

As can be seen in the left panel of the figure, the variation of the mass of the CQM pole with  $c_1$  is quite mild within the cutoff scheme. It changes only about 3 MeV,  $M_{\text{CQM}} \in [2614.7, 2617.8]$  MeV, when  $c_1$  varies in the  $[-2.0, 0.5]$  interval and, at most,  $M_{\text{CQM}}$  reaches values close to 2630 MeV for the largest positive values of  $c_1$  shown in the figure. At the same time  $|g_{\Sigma_c^* \pi}|$  goes from 1.3 down to 0.8 when  $c_1$  varies from  $-3$  to 2. Hence, one can accommodate the experimental mass in the region of 2628 MeV consistently with the upper bound on the  $\Sigma_c^*$ -resonant contribution to the width discussed in Eq. (23). The molecular probability of this state would be small since  $P_{\Sigma_c^* \pi} \sim 0.1$ , reaching maximum values of about 0.2, when  $c_1$  is close to  $-3$ . Moreover, for this latter value of  $c_1$ ,  $P_{ND^*}$ , defined analogously to  $P_{\Sigma_c^* \pi}$  in Eq. (24) with the obvious replacements, is of the order of 0.04. When  $c_1$  increases,  $P_{ND^*}$  (not shown in the plot) continues decreasing and it becomes zero close to  $c_1 = 0.2$ . From this point,  $P_{ND^*}$  starts growing to reach values of the order of 0.08 for  $c_1 = 2$ . The coupling  $|g_{ND^*}|$ , displayed in the figure, follows a similar pattern, as expected.

Results obtained within the  $SC\mu$  scheme, shown in the right panel of Fig. 4, differ from those discussed above, but some qualitative features are similar: the  $P_{ND^*}$  and  $|g_{ND^*}|$  behaviors, the small molecular probability and the mild dependence of  $M_{\text{CQM}}$  and  $|g_{\Sigma_c^* \pi}|$  on  $c_1$ . The maximum values obtained for the mass ( $\sim 2618$ ) of the state are

found for  $c_1$  in the region of  $-0.8$ . Note, however, that the possible tension with the experimental mass of 2628.11 MeV is not really significant, since the agreement can be likely improved by changing the renormalization parameter  $\alpha$ .

In Table I, we present together the properties of CQM and molecular  $J^P = 3/2^-$  poles, for  $d_1 = -0.8$  and  $c_1 = 0, 1$ , and  $-1$ , and both renormalization schemes. The dressed CQM results of the table were already discussed in Fig. 4. The properties of the molecular state, which would have  $j_{\text{ldof}}^\pi = 1^-$  quantum numbers, hardly depend on  $c_1$  and both renormalization schemes predict a new state around 2.7 GeV and 60 MeV of width. The emergence of this new resonance, which would not be the  $\Lambda_c(2625)$ , can be clearly seen in the FRS and SRS plots of Fig. 5, where larger values of  $|c_1|$  than in Table I have been considered.

Hence, we conclude that the physical  $\Lambda_c(2625)$  finds naturally its origin in the CQM bare state obtained in Ref. [8], while we predict the existence of a molecular baryon, moderately broad, with a mass of about 2.7 GeV and sizable couplings to both  $\Sigma_c^* \pi$  and  $ND^*$ .

This latter pole will not show up in the experimental  $\Lambda_c \pi \pi$  spectrum, dominated by the physical resonance. Furthermore, this state, mistakenly associated with the  $\Lambda_c(2625)$  in the previous  $SU(6)_{\text{lsf}} \times \text{HQSS}$  studies of Refs. [20,21] where the coupling to CQM d.o.f. was not considered, will be similar to that found in the chiral



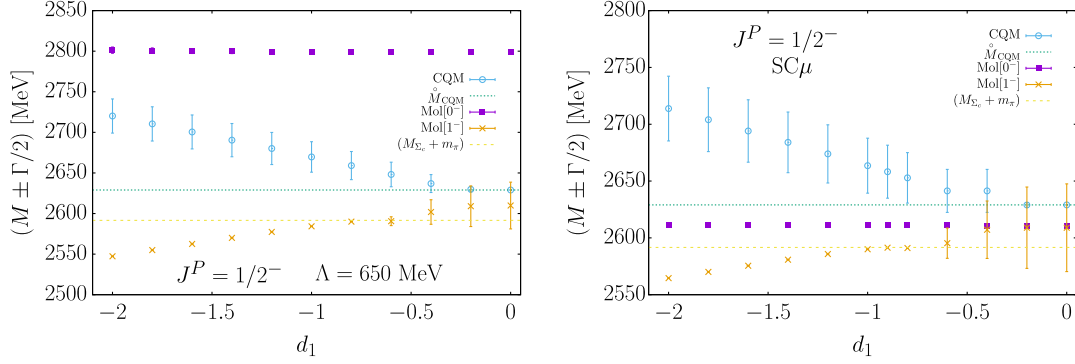


FIG. 6. Dependence of the  $J^P = 1/2^-$  CQM and molecular pole positions as a function of the LEC  $d_1$ , for  $c_1 = 0$ . We show results for both, the cutoff and  $SC\mu$  ( $\alpha = 0.95$ ) renormalization schemes, and the values of the bare CQM mass and the  $\Sigma_c\pi$  threshold energy. Molecular states are labeled according to their dominant  $ldof$  configuration,  $0^-$  or  $1^-$ .

approach of Ref. [18] or to the  $\Sigma_c^*\pi$  pole reported in the ELHG scheme followed<sup>7</sup> in [29]. The SU(3) chiral approach of Ref. [15] reduces the mass of this molecular state down to that of the  $\Lambda_c(2625)$  by using a large UV cutoff of 2.13 GeV. This points, following the arguments given in [55,56], to the existence of some relevant d.o.f. (CQM states and/or  $ND^*$  components) that are not properly accounted for in [15].

## 2. The $\Lambda_c(2595)$

Now, we turn the discussion into the  $J^P = 1/2^-$  sector. As we did before, in a first stage we set  $c_1$  to zero and start varying  $d_1$ . Results are depicted in Fig. 6. There appear now three poles for both renormalization schemes considered in this work. As compared to the case in the left panels of Fig. 2, where the coupling between CQM and baryon-meson d.o.f. was switched off, there is an extra state which has its origin in the  $j_{ldof}^\pi = 1^-$  CQM bare state. The mass and the width of the narrow state at 2800 MeV ( $\Lambda = 650$  MeV) or 2610 MeV ( $SC\mu$ ) are practically unaltered by  $d_1$ . This is a trivial consequence of the largely dominant  $j_{ldof}^\pi = 0^-$  configuration of these states, since HQSS forbids their coupling to the  $j_{ldof}^\pi = 1^-$  CQM bare state.

The location of the second broad molecular state,  $[\Lambda_{c(b)}^{1^-}(2595)]$ , observed in Fig. 2, is strongly influenced by the quark-model state that produces an attraction that grows with  $d_1^2$ . Thus, for  $d_1 < -0.6$  or  $-0.7$ , depending on the renormalization procedure, it moves below the  $\Sigma_c\pi$  threshold and becomes a bound state. Within the  $SC\mu$  scheme, this  $j_{ldof}^\pi = 1^-$  molecular state would not be, however, identified with the physical  $\Lambda_c(2595)$  resonance

that would be reproduced by the narrow  $\Lambda_{c(n)}^{0^-}$  (2595) pole at 2610–2611 MeV, with small  $|g_{\Sigma_c\pi}|$  coupling<sup>8</sup> and large  $|g_{ND^*}|$  and  $|g_{ND^*}|$  ones, especially the latter ( $\geq 6.2$ ). The situation is different in the UV cutoff scheme, since the  $j_{ldof}^\pi = 0^-$  narrow resonance is placed at 2800 MeV, and it is precisely the  $j_{ldof}^\pi = 1^-$  molecular state, the best candidate to describe the physical  $\Lambda_c(2595)$ .

In addition, we see in Fig. 6 that the bare CQM state is modified due to the baryon-meson loop effects, and it is moved to the complex plane acquiring also a finite width that obviously grows with  $d_1^2$ . The quantitative details, nevertheless, depend on the renormalization scheme.

As in the  $\Lambda_c(2625)$  subsection, we fix  $d_1 = -0.8$  from the CQM of Ref. [12], and study in Table II and Fig. 7, the dependence of the spectrum of states on the LEC  $c_1$ . As expected, the mass position of the  $j_{ldof}^\pi = 0^-$  pole is hardly affected, while its small width depends much more on  $c_1$ . As mentioned above, within the  $SC\mu$  scheme, the physical  $\Lambda_c(2595)$  is identified with the  $\Lambda_{c(n)}^{0^-}$  (2595). We see that the pole might have a coupling to the  $\Sigma_c\pi$  pair that is smaller than 1, and thus it would be smaller than needed to reproduce the experimental width from Eq. (18). In the UV cutoff approach, instead, there would be a molecular narrow state close to the  $ND$  threshold, strongly coupled to it and that might provide some visible signatures in processes involving final state interactions of this baryon-meson pair (see bottom panels of Fig. 7). In this latter renormalization scheme, the  $\Lambda_c(2595)$  is described by the  $j_{ldof}^\pi = 1^-$  hadron molecule located below threshold at around 2590 MeV, little affected by  $c_1$ , and with  $|g_{\Sigma_c\pi}| \sim 1$ . Thus, from Eq. (18) the  $\Lambda_c(2595) \rightarrow \Lambda\pi\pi$  width will be predicted to be around 1.8, in good agreement with experiment ( $2.6 \pm 0.6$ ). Nevertheless, the  $\Lambda_c(2595)$ , despite of having  $1^-$  quantum numbers for the  $ldof$ , would not be the HQSS partner of the  $\Lambda_c(2625)$  either in this case,

<sup>7</sup>In that work, it was not identified with the  $\Lambda_c(2625)$  resonance, which is generated there as an  $ND^*$  state, after modifying the ELHG  $ND^* \rightarrow ND^*$  potential including box-diagrams constructed out of the anomalous  $D^*D^*\pi$  coupling, and fitting the UV cutoffs to reproduce its mass.

<sup>8</sup>It decreases with  $d_1^2$  and it varies from 0.5 for  $d_1 = 0$  down to 0.04 for  $d_1 = -2$ .

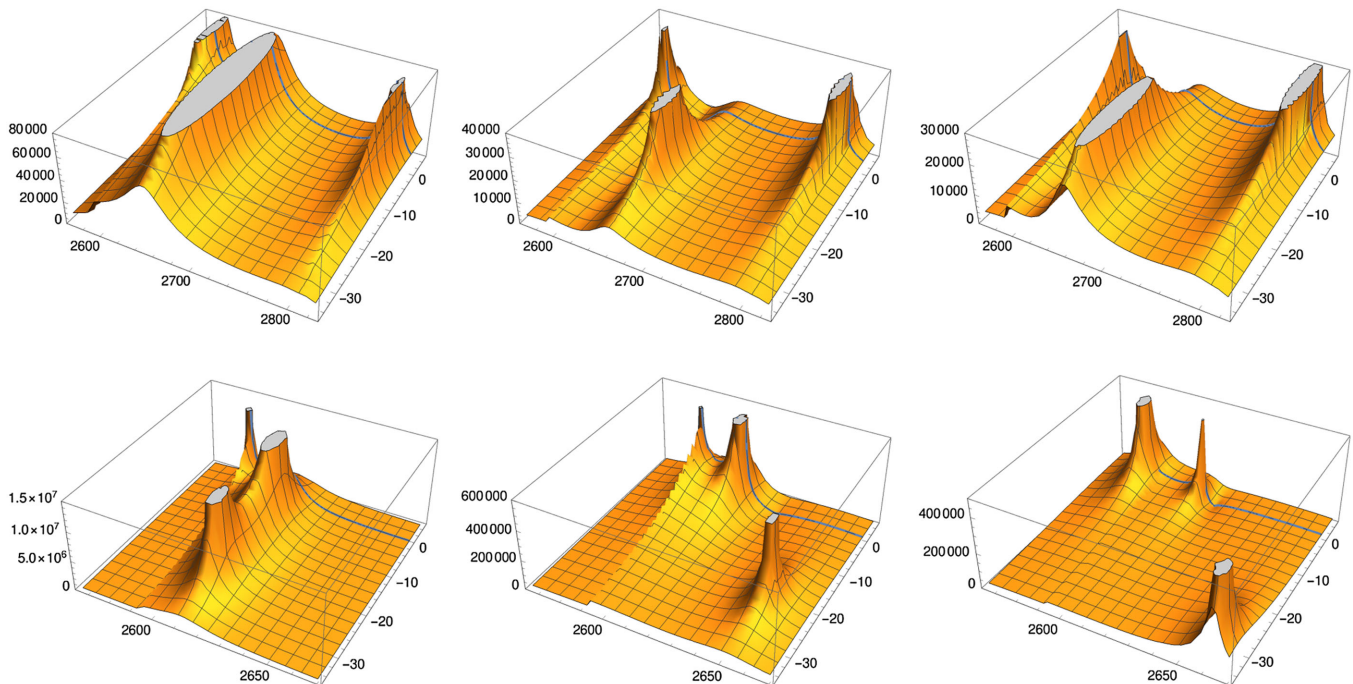


FIG. 7. AVD- $T$  in the  $J^P = 1/2^-$  sector using two UV renormalization schemes:  $SC\mu$  ( $\alpha = 0.95$ ) and a cutoff of 650 MeV in the bottom and top panels, respectively, for different CQM and baryon-meson pair couplings (from left to right):  $(c_1 = -3, d_1 = -0.8)$ ,  $(c_1 = 0, d_1 = -0.8)$ , and  $(c_1 = 2, d_1 = -0.8)$ . We display the AVD- $T$  for both the FRS [ $\text{Im}(E) > 0$ ] and the SRS [ $\text{Im}(E) < 0$ ] [fm] of the unitarized amplitudes as a function of the complex energy  $E$  [MeV]. We also show the scattering line (blue solid curve) in all the cases. Note that the range of  $\text{Re}(E)$  is much larger in the top panels than in the bottom ones. Axes are defined as in Fig. 2.

because of the predominantly quark-model structure of the latter. Indeed, the  $\Lambda_c(2595)$  would have a large molecular content,  $P_{\Sigma_c^* \pi} = 0.6-0.7$ .

Note that the  $j_{1\text{dof}}^\pi = 1^-$  state in the  $SC\mu$  scheme will be irrelevant, since its effects will be completely overcome by those produced by the  $\Lambda_{c(n)}^{0-}(2595)$  (see Fig. 7); independently it is placed below the  $\Sigma_c \pi$  threshold or it becomes a broad resonance.

The different inner structure of the  $\Lambda_c(2595)$  within the UV cutoff and  $SC\mu$  schemes and the dependence of this structure on  $c_1$  will lead to differences in  $ND$  and  $ND^*$  couplings that would produce different predictions for the exclusive semileptonic  $\Lambda_b \rightarrow \Lambda_c(2595)$  decay [37,50].

Finally, we see that in both renormalization schemes we obtain the dressed CQM pole at masses around 2640–2660 MeV and with a width of the order of 30–50 MeV, depending on the chosen regulator and on  $c_1$ , though for moderate variations, one should not expect a large dependence on  $c_1$  because the  $ND$  and  $ND^*$  thresholds are not too close. This is a prediction of the present work, and this state should provide signatures in the open channel  $\Sigma_c \pi$  since its coupling to this pair is sizable, well above one. As seen in Fig. 7, for large negative values<sup>9</sup> of  $c_1$  in the  $SC\mu$  case, it could, however, be shadowed by the  $\Lambda_{c(n)}^{0-}(2595)$  resonance.

<sup>9</sup>What it is really relevant is that the product  $c_1 d_1$  is positive.

### C. Further comments

Here, we briefly revisit and summarize some of the features/assumptions of the current approach that induce ambiguities in the main conclusions of this work, which we will be collected in the next section. We also suggest, when possible, how the model dependence can be fixed by future measurements.

- (i) The regularization of the loop function determines the off-shell behaviors of the amplitudes and leads to a model dependence, as we have put here to demonstrate by comparing the  $SC\mu$  and UV cutoff results. This source of systematic errors is ignored in most of the molecular approaches available in the literature. The existence of a narrow  $J^P = 1/2^-$  state close to the  $ND$  threshold would disentangle between these two renormalization schemes, since it will definitely favor the UV cutoff scheme. This state would show up in the  $\Sigma_c \pi$  spectrum through virtual  $ND$  and  $ND^*$  loops.
- (ii) The LECs  $c_1$  and  $d_1$  that control the interplay between the bare CQM and the baryon-meson d.o.f. are uncertain and are UV renormalization scheme-dependent parameters. Nevertheless, the results displayed in Fig. 3 for the  $J^P = 3/2^-$  higher mass resonance constrain considerably  $d_1$  (coupling between the bare CQM state and  $\Sigma_c \pi$ ). We find a sizable dependence of the mass of this state on  $d_1$  that can

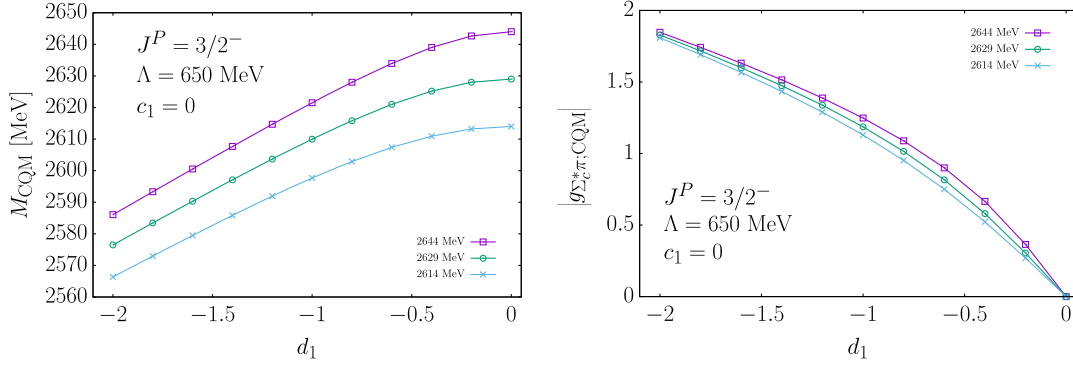


FIG. 8. Mass (left) and coupling to  $\Sigma_c^* \pi$  (right) of the dressed CQM state as a function of the LEC  $d_1$ , for three different values of the mass of the bare CQM state,  $\overset{\circ}{M}_{\text{CQM}} = 2544, 2529$ , and  $2514$  MeV, in the  $J^P = 3/2^-$  sector. In addition, the LEC  $c_1$  has been fixed to zero. We show results obtained with the cutoff renormalization scheme.

serve to fix this LEC in both renormalization schemes employed in this work. Interestingly, we also observe that the mass and the width of this resonance do not depend drastically on the regularization method. We note that the range of values considered in Fig. 3 for  $|d_1|$  is sufficiently large, given that it is estimated to be around 0.8 in Ref. [12], using a framework compatible with the CQM employed in [8] from which we have taken  $\overset{\circ}{M}_{\text{CQM}}$ . Hence, we end up with a reasonably robust prediction for the existence of a  $J^P = 3/2^-$  molecular baryon, moderately broad ( $\Gamma \sim 60$  MeV), with a mass of about 2.7 GeV and sizable couplings to both  $\Sigma_c^* \pi$  and  $ND^*$ . The future observation of this resonance, additional to the  $\Lambda_c(2625)$ , would greatly limit the possible values of  $d_1$ .

The results shown in Fig. 3 were obtained for  $c_1 = 0$ , i.e., a vanishing coupling between the bare CQM state and the  $j_{\text{ldof}}^\pi = 1^-$ -component of the  $ND^*$  pair. Nevertheless, moderate nonzero values of this LEC do not modify appreciably the mass and the width of the higher  $J^P = 3/2^-$  resonance, as seen in Table I. This is because this state is placed significantly far from the  $ND^*$  threshold. Indeed, most of the results found in this work are a little sensitive to  $c_1$ , because the  $ND$  and  $ND^*$  thresholds are far from  $\overset{\circ}{M}_{\text{CQM}}$ , mass of the bare three-quark state with  $j_{\text{ldof}}^\pi = 1^-$ , and in addition, the former meson-baryon pairs feel the strongest interaction in the  $j_{\text{ldof}}^\pi = 0^-$  channel, as discussed in Sec. II. This reduced dependence on  $c_1$  certainly make our results more robust.<sup>10</sup>

- (iii) The CQM  $j_{\text{ldof}}^\pi = 1^-$  bare mass,  $\overset{\circ}{M}_{\text{CQM}}$ , is also an UV renormalization scheme-dependent parameter in

our approach. We have fixed it to the value obtained in the state of the art CQM calculation of Ref. [8]. There, single- and double-heavy baryons were studied, with model parameters fixed by the strange baryon spectra, finding that the predictions for the masses of the observed charmed and bottomed baryons turned out to be in a fairly good agreement with experiment. The predictions for the  $\Lambda_c(2625)$  are the most sensitive to the choice of  $\overset{\circ}{M}_{\text{CQM}}$ , but even in this case, the properties of this resonance are reasonably stable in front of moderate variations of the mass of the bare CQM state, as can be seen in Fig. 8. In this latter figure, we show the produced changes in the mass (left) and coupling to  $\Sigma_c^* \pi$  (right) of the dressed  $J^P = 3/2^-$  CQM state, as a function of the LEC  $d_1$ , when  $\overset{\circ}{M}_{\text{CQM}}$  is shifted by  $\pm 15$  MeV with respect to the value of 2529 MeV used here and taken from [8]. We see that as  $|d_1|$  increases the effect on the mass of the dressed state decreases. The  $J^P = 3/2^-$  higher mass resonance, located in the region of 2.7 GeV, is much less affected and for the largest  $|d_1| = 2$  coupling, its mass changes only at the level of 5 MeV, while it becomes 2–3 MeV wider (narrower) when  $\overset{\circ}{M}_{\text{CQM}} = 2614(2644)$  MeV is employed. These variations are comparable to those produced by  $c_1$ , as mentioned above.

#### IV. CONCLUSIONS

We have shown that the  $\Lambda_c(2595)$  and the  $\Lambda_c(2625)$  are not HQSS partners. The  $J^P = 3/2^-$  resonance should be viewed mostly as a quark-model state naturally predicted to lie very close to its nominal mass [8]. This contradicts a large number of molecular scenarios suggested for this resonance in the literature. In addition, there will exist a molecular baryon, moderately broad, with a mass of about

<sup>10</sup>In any case as we mentioned, the position of the  $J^P = 1/2^-$  poles show a certain dependence for very large values of  $c_1$  (see Fig. 7), which might be used to constrain this LEC.



2.7 GeV and sizable couplings to both  $\Sigma_c^* \pi$  and  $ND^*$ , which will fit into the expectations of being a  $\Sigma_c^* \pi$  molecule generated by the chiral interaction of this pair.

The  $\Lambda_c(2595)$  is predicted, however, to have a predominant molecular structure. This is because it is either the result of the chiral  $\Sigma_c \pi$  interaction, whose threshold is located much closer than the mass of the bare three-quark state, or because the  $ldof$  in its inner structure are coupled to the unnatural  $0^-$  quantum numbers. The latter is what happens in the  $SC\mu$  renormalization scheme that enhances the influence of the  $ND^*$  channel in the dynamics of this narrow resonance. Attending to the three-body  $\Lambda_c(2595) \rightarrow \Lambda \pi \pi$  decay width, the  $SC\mu$  scenario is slightly disfavored, and it looks more natural to assign a  $1^-$  configuration to the  $ldof$  content of the physical  $\Lambda_c(2595)$  state, as found when an UV cutoff is employed.

We also obtain a further  $J^P = 1/2^-$  resonance that is the result of dressing the bare CQM pole with baryon-meson loops. It would have a mass of around 2640–2660 MeV and a width of the order of 30–50 MeV. Finally, within the UV cutoff renormalization scheme, we also find a narrow state at 2800 MeV close to the  $ND$  threshold. This state has large  $ND$  and  $ND^*$  couplings and it should provide some visible signatures in processes involving final state interactions of the  $ND$  and  $ND^*$  pairs.

The spectrum found in this work cannot be easily understood in terms of HQSS, despite having used interactions that respect this symmetry. This is because the bare

quark-model state and the  $\Sigma_c \pi$  threshold are located extraordinarily close to the  $\Lambda_c(2625)$  and  $\Lambda_c(2595)$ , respectively, and hence they play totally different roles in each sector. Note that  $(M_{\Sigma_c^*} - M_{\Sigma_c}) \sim 65$  MeV is around a factor of 2 larger than the  $\Lambda_c(2625) - \Lambda_c(2595)$  mass splitting. This does not fit well into a molecular picture of these two resonances generated by  $\Sigma_c^{(*)} \pi$  chiral forces and, in addition, the splitting found in the CQM study of Ref. [8] is only of 2 MeV, much smaller than any of the mass differences quoted above. Moreover, the  $SC\mu$  renormalization scheme leads to an unexpected enhancing of the importance of the  $j_{ldof}^\pi = 0^-$  components of the  $SU(6)_{\text{lsf}} \times \text{HQSS}$  interaction in the  $J^P = 1/2^-$  sector, which are driven by  $ND - ND^*$  coupled-channels interactions. This is not the case when an UV cutoff is employed.

## ACKNOWLEDGMENTS

R. P. Pavao wishes to thank the program Santiago Grisolia of the Generalitat Valenciana. This research has been supported by the Spanish Ministerio de Ciencia, Innovación y Universidades and European FEDER funds under Contracts No. FIS2017-84038-C2-1-P and No. SEV-2014-0398. This project has received funding from the European Unions Horizon 2020 research and innovation programme under Grant agreement No. 824093.

- 
- [1] N. Isgur and M. B. Wise, *Phys. Rev. Lett.* **66**, 1130 (1991).
  - [2] M. B. Wise, *Phys. Rev. D* **45**, R2188 (1992).
  - [3] M. Neubert, *Phys. Rep.* **245**, 259 (1994).
  - [4] L. Copley, N. Isgur, and G. Karl, *Phys. Rev. D* **20**, 768 (1979).
  - [5] S. Migura, D. Merten, B. Metsch, and H.-R. Petry, *Eur. Phys. J. A* **28**, 41 (2006).
  - [6] H. Garcilazo, J. Vijande, and A. Valcarce, *J. Phys. G* **34**, 961 (2007).
  - [7] W. Roberts and M. Pervin, *Int. J. Mod. Phys. A* **23**, 2817 (2008).
  - [8] T. Yoshida, E. Hiyama, A. Hosaka, M. Oka, and K. Sadato, *Phys. Rev. D* **92**, 114029 (2015).
  - [9] N. Isgur, M. B. Wise, and M. Youssefmir, *Phys. Lett. B* **254**, 215 (1991).
  - [10] M. Tanabashi *et al.* (Particle Data Group), *Phys. Rev. D* **98**, 030001 (2018).
  - [11] H. Nagahiro, S. Yasui, A. Hosaka, M. Oka, and H. Noumi, *Phys. Rev. D* **95**, 014023 (2017).
  - [12] A. Arifi, H. Nagahiro, and A. Hosaka, *Phys. Rev. D* **95**, 114018 (2017).
  - [13] M. Lutz and E. Kolomeitsev, *Nucl. Phys. A* **730**, 110 (2004).
  - [14] L. Tolos, J. Schaffner-Bielich, and A. Mishra, *Phys. Rev. C* **70**, 025203 (2004).
  - [15] J.-X. Lu, Y. Zhou, H.-X. Chen, J.-J. Xie, and L.-S. Geng, *Phys. Rev. D* **92**, 014036 (2015).
  - [16] J. Hofmann and M. Lutz, *Nucl. Phys. A* **763**, 90 (2005).
  - [17] T. Mizutani and A. Ramos, *Phys. Rev. C* **74**, 065201 (2006).
  - [18] J. Hofmann and M. F. M. Lutz, *Nucl. Phys. A* **776**, 17 (2006).
  - [19] C. E. Jimenez-Tejero, A. Ramos, and I. Vidana, *Phys. Rev. C* **80**, 055206 (2009).
  - [20] C. Garcia-Recio, V. K. Magas, T. Mizutani, J. Nieves, A. Ramos, L. L. Salcedo, and L. Tolos, *Phys. Rev. D* **79**, 054004 (2009).
  - [21] O. Romanets, L. Tolos, C. Garcia-Recio, J. Nieves, L. Salcedo, and R. Timmermans, *Phys. Rev. D* **85**, 114032 (2012).
  - [22] J. Oller and U. G. Meissner, *Phys. Lett. B* **500**, 263 (2001).
  - [23] C. Garcia-Recio, J. Nieves, E. Ruiz Arriola, and M. J. Vicente Vacas, *Phys. Rev. D* **67**, 076009 (2003).
  - [24] T. Hyodo, S. Nam, D. Jido, and A. Hosaka, *Phys. Rev. C* **68**, 018201 (2003).
  - [25] D. Jido, J. Oller, E. Oset, A. Ramos, and U. Meissner, *Nucl. Phys. A* **725**, 181 (2003).



- [26] C. Garcia-Recio, M. F. M. Lutz, and J. Nieves, *Phys. Lett. B* **582**, 49 (2004).
- [27] T. Hyodo and D. Jido, *Prog. Part. Nucl. Phys.* **67**, 55 (2012).
- [28] Y. Kamiya, K. Miyahara, S. Ohnishi, Y. Ikeda, T. Hyodo, E. Oset, and W. Weise, *Nucl. Phys.* **A954**, 41 (2016).
- [29] W. Liang, T. Uchino, C. Xiao, and E. Oset, *Eur. Phys. J. A* **51**, 16 (2015).
- [30] M. Bando, T. Kugo, S. Uehara, K. Yamawaki, and T. Yanagida, *Phys. Rev. Lett.* **54**, 1215 (1985).
- [31] M. Bando, T. Kugo, and K. Yamawaki, *Phys. Rep.* **164**, 217 (1988).
- [32] U. G. Meissner, *Phys. Rep.* **161**, 213 (1988).
- [33] C. Xiao, J. Nieves, and E. Oset, *Phys. Rev. D* **88**, 056012 (2013).
- [34] V. Baru, C. Hanhart, Yu. S. Kalashnikova, A. E. Kudryavtsev, and A. V. Nefediev, *Eur. Phys. J. A* **44**, 93 (2010).
- [35] E. Cincioglu, J. Nieves, A. Ozpineci, and A. U. Yilmazer, *Eur. Phys. J. C* **76**, 576 (2016).
- [36] C. Garcia-Recio, J. Nieves, O. Romanets, L. Salcedo, and L. Tolos, *Phys. Rev. D* **87**, 074034 (2013).
- [37] J. Nieves, R. Pavao, and S. Sakai, *Eur. Phys. J. C* **79**, 417 (2019).
- [38] J. Nieves and E. Ruiz Arriola, *Phys. Rev. D* **64**, 116008 (2001).
- [39] C. Garcia-Recio, L. S. Geng, J. Nieves, and L. L. Salcedo, *Phys. Rev. D* **83**, 016007 (2011).
- [40] M. Albaladejo, P. Fernandez-Soler, J. Nieves, and P. G. Ortega, *Eur. Phys. J. C* **77**, 170 (2017).
- [41] M. Albaladejo, P. Fernandez-Soler, J. Nieves, and P. G. Ortega, *Eur. Phys. J. C* **78**, 722 (2018).
- [42] D. Gamermann, C. Garcia-Recio, J. Nieves, and L. L. Salcedo, *Phys. Rev. D* **84**, 056017 (2011).
- [43] P. L. Cho, *Phys. Rev. D* **50**, 3295 (1994).
- [44] D. Pirjol and T.-M. Yan, *Phys. Rev. D* **56**, 5483 (1997).
- [45] H. Albrecht *et al.* (ARGUS Collaboration), *Phys. Lett. B* **317**, 227 (1993).
- [46] T. Aaltonen *et al.* (CDF Collaboration), *Phys. Rev. D* **84**, 012003 (2011).
- [47] H. Albrecht *et al.* (ARGUS Collaboration), *Phys. Lett. B* **402**, 207 (1997).
- [48] P. L. Frabetti *et al.* (E687 Collaboration), *Phys. Lett. B* **365**, 461 (1996).
- [49] K. W. Edwards *et al.* (CLEO Collaboration), *Phys. Rev. Lett.* **74**, 3331 (1995).
- [50] W.-H. Liang, E. Oset, and Z.-S. Xie, *Phys. Rev. D* **95**, 014015 (2017).
- [51] S. Weinberg, *Phys. Rev.* **130**, 776 (1963).
- [52] S. Weinberg, *Phys. Rev.* **137**, B672 (1965).
- [53] D. Gamermann, J. Nieves, E. Oset, and E. Ruiz Arriola, *Phys. Rev. D* **81**, 014029 (2010).
- [54] C. Garcia-Recio, C. Hidalgo-Duque, J. Nieves, L. L. Salcedo, and L. Tolos, *Phys. Rev. D* **92**, 034011 (2015).
- [55] F.-K. Guo, U.-G. Meissner, and B.-S. Zou, *Commun. Theor. Phys.* **65**, 593 (2016).
- [56] M. Albaladejo, J. Nieves, E. Oset, Z.-F. Sun, and X. Liu, *Phys. Lett. B* **757**, 515 (2016).